ITWM

Fraunhofer Institut
Techno- und
Wirtschaftsmathematik

V. Rutka, A. Wiegmann

Explicit Jump Immersed Interface Method for virtual material design of the effective elastic moduli of composite materials

Vorwort

Das Tätigkeitsfeld des Fraunhofer Instituts für Techno- und Wirtschaftsmathematik ITWM umfasst anwendungsnahe Grundlagenforschung, angewandte Forschung sowie Beratung und kundenspezifische Lösungen auf allen Gebieten, die für Techno- und Wirtschaftsmathematik bedeutsam sind.

In der Reihe »Berichte des Fraunhofer ITWM« soll die Arbeit des Instituts kontinuierlich einer interessierten Öffentlichkeit in Industrie, Wirtschaft und Wissenschaft vorgestellt werden. Durch die enge Verzahnung mit dem Fachbereich Mathematik der Universität Kaiserslautern sowie durch zahlreiche Kooperationen mit internationalen Institutionen und Hochschulen in den Bereichen Ausbildung und Forschung ist ein großes Potenzial für Forschungsberichte vorhanden. In die Berichtreihe sollen sowohl hervorragende Diplom- und Projektarbeiten und Dissertationen als auch Forschungsberichte der Institutsmitarbeiter und Institutsgäste zu aktuellen Fragen der Techno- und Wirtschaftsmathematik aufgenommen werden.

Darüberhinaus bietet die Reihe ein Forum für die Berichterstattung über die zahlreichen Kooperationsprojekte des Instituts mit Partnern aus Industrie und Wirtschaft.

Berichterstattung heißt hier Dokumentation darüber, wie aktuelle Ergebnisse aus mathematischer Forschungs- und Entwicklungsarbeit in industrielle Anwendungen und Softwareprodukte transferiert werden, und wie umgekehrt Probleme der Praxis neue interessante mathematische Fragestellungen generieren.

Prof. Dr. Dieter Prätzel-Wolters
Institutsleiter

Kaiserslautern, im Juni 2001

Explicit Jump Immersed Interface Method for virtual material design of the effective elastic moduli of composite materials

Vita Rutka[*]   Andreas Wiegmann[†]

February 23, 2005

Abstract

Virtual material design is the microscopic variation of materials in the computer, followed by the numerical evaluation of the effect of this variation on the material's macroscopic properties. The goal of this procedure is an in some sense improved material. Here, we give examples regarding the dependence of the effective elastic moduli of a composite material on the geometry of the shape of an inclusion. A new approach on how to solve such interface problems avoids mesh generation and gives second order accurate results even in the vicinity of the interface.

The Explicit Jump Immersed Interface Method is a finite difference method for elliptic partial differential equations that works on an equidistant Cartesian grid in spite of non-grid aligned discontinuities in equation parameters and solution. Near discontinuities, the standard finite difference approximations are modified by adding correction terms that involve jumps in the function and its derivatives. This work derives the correction terms for two dimensional linear elasticity with piecewise constant coefficients, i.e. for composite materials. It demonstrates numerically convergence and approximation properties of the method.

Keywords: virtual material design, explicit jump immersed interface method, effective elastic moduli, composite materials

1   Introduction

Modern composite materials are designed to have all the good properties of their constituents while avoiding the bad ones. For example, light and strong materials can be manufactured by reinforcing a lighter matrix material with properly oriented heavier and stronger fibers. Virtual material design is the microscopic variation of materials in the computer, followed by the numerical

---

[*]Fraunhofer ITWM Kaiserslautern and University of Kaiserslautern, Department of Mathematics. E-mail: `rutka@itwm.fraunhofer.de`

[†]Fraunhofer ITWM Kaiserslautern. E-mail: `wiegmann@itwm.fraunhofer.de`

evaluation of the effect of this variation on the material's macroscopic proper-
ties. The goal of this procedure is an in some sense improved material. How-
ever, the numerical solution of elliptic equations with discontinuous coefficients
continues to be a challenge to the mathematics and engineering communities
to this day. The Immersed Interface method by Li and LeVeque [3] is one
approach to deal with such discontinuities. The ability to solve interface prob-
lems even for large contrast cases, i.e. when the quotient between coefficients
on the two sides of the interface is large, was achieved after some modifications
to the original IIM, [4, 12], and is notably the main reason for the existence
of the Explicit jump version. The availability of a fast solution methodology
for boundary value problems, and the fact that the Explicit Jump Immersed
Interface Method does not require any grid generation lead to the use of the
EJIIM for elastostatic design problems in [10]. Such problems are characterized
by the fact that the equations of linear elasticity need to be solved repeatedly
in quite complicated geometries. These geometries vary from one design step
to the next, and avoiding mesh generation between elastostatic solves is a huge
advantage.

The current work on EJIIM for composite materials was begun in [7] for several
reasons. The explicit treatment of the interface conditions allows to naturally
deal with any boundary conditions that might be appropriate at the interface.
Because cracks ususally start at points of high stress and these in turn often
occur near the interface, the second order quality of the solution even at the
interface is attractive. And last but not least, because we are interested in
designing the material, thus in many solutions on varying geometries, avoiding
mesh generation is a great advantage. In fact, the second order discretization
for composite materials in 2d is completed in the Appendix of this paper, and
work for porous materials in 3d is under way [9], together with more analytical
work in [8]. What is still missing from completely achieving a great method
for virtual composite material design is the fact that the fast iterative solver
technologies from the Poisson-type equations [4, 12] and boundary value type
problems for linear elasticity [11] could not yet be carried over to the composite
material elastostatic case [7]. This lack of a fast iterative solver is the reason
why this work is currently only feasible in 2d in terms of computation time. We
now believe that multigrid and adaptive techniques will be needed to reach the
solution speed previously achieved by the EJIIM discretization approch coupled
with FFT-based fast solvers [11] while keeping the solution quality that results
from the second order discretization.

In §2 we summarize the equations of isotrope linear elasticity (Navier or Lamé
equations) in a bounded domain and analytic jump conditions at a material
interface. §3 gives the principle ideas of the Explicit Jump Immersed Interface
Method. The next §4 illustrates the second order convergence of the approach
and compares with previous numerical results. In §5, the dependence of the
effective elastic moduli of the material on the variation of the geometry of the
inclusion is illustrated by examples. We conclude with §6.

2 Model Equations

We consider the equations of isotrope linear elasticity (Navier or Lamé equations) in a bounded domain $\Omega \in \mathbb{R}^2$ with sufficiently smooth boundary:

$$\mu\Delta\mathbf{u} + (\mu + \lambda)\nabla\nabla \cdot \mathbf{u} = \mathbf{f} \ . \tag{1}$$

$\mathbf{f} : \Omega \to \mathbb{R}^2$ is the body force and $\mathbf{u} = (u, v)^T$ is the displacement vector. μ and λ are Lamé moduli. The stress tensor is

$$\boldsymbol{\sigma} = \begin{pmatrix} \sigma_{xx} & \sigma_{xy} \\ \sigma_{xy} & \sigma_{yy} \end{pmatrix} := \mu \left(\nabla\mathbf{u} + (\nabla\mathbf{u})^T \right) + \lambda \begin{pmatrix} \partial_x & 0 \\ 0 & \partial_y \end{pmatrix} \mathbf{u} \ .$$

The boundary conditions are given as prescribed displacements $\mathbf{u} = \mathbf{u}_\Gamma$ on $\partial\Omega_D$ or by acting tractions $\boldsymbol{\sigma}\mathbf{n} = \mathbf{S}$ on $\partial\Omega_T$, where $\mathbf{n}$ is the outer normal to Ω. We require $\partial\Omega_D \cup \partial\Omega_T = \partial\Omega$, $\partial\Omega_D \cap \partial\Omega_T = \emptyset$ and length$(\partial\Omega_D) \geq \delta > 0$ and consider a situation when μ and λ are piecewise constant functions. This models a composite consisting of homogeneous isotrope phases. To easiest write the conditions of perfect contact we consider the divergence form of the equilibrium equation (1):

$$\nabla \cdot \begin{pmatrix} (2\mu + \lambda)u_x + \lambda v_y & \mu(u_y + v_x) \\ \mu(u_y + v_x) & \lambda u_x + (2\mu + \lambda)v_y \end{pmatrix} = \mathbf{f} \ . \tag{2}$$

To keep things sikmple, we consider only two phases, occupying domains Ω^+ and Ω^-, $\Omega = \Omega^+ \cup \Omega^-$ with coefficients λ^+, μ^+ and λ^- and μ^- respectively. The coefficients λ and μ are discontinuous along some sufficiently smooth *interface* Γ that does not intersect the boundary of the computational domain.

At Γ we have the interface conditions

$$[\mathbf{u}] = \bar{\mathbf{u}} \tag{3}$$
$$[\boldsymbol{\sigma}\mathbf{n}] = \mathbf{g} \ . \tag{4}$$

In the case of perfect contact (2), $\bar{\mathbf{u}} = 0$ and $\mathbf{g} = 0$. Here by $[.]$ we denote the jumps, i.e.,

$$[p(P)] := p^+(P) - p^-(P)$$

for some function p and

$$p^\pm(P) := \lim_{\substack{\mathbf{x} \to P \\ \mathbf{x} \in \Omega^\pm}} p(\mathbf{x}) \ .$$

Note that if $\bar{\mathbf{u}}$ is not zero, this term enters (2) as dipole source along Γ and that if $\mathbf{g}$ is not zero, it enters (2) as delta source along Γ .

3 The principle ideas of EJIIM

As one of the extensions of the original Immersed Interface Method [3], the EJIIM was developed for Poisson-type equations in [12]. In [10], the EJIIM

was developed for the linear elastic case boundary value problem that arises by embedding an irregularly shaped object in a rectangle, and the EJIIM and the Level Set Method [6] were used for optimal shape design with respect to plane stress/strain problems for domains with non-grid aligned boundaries but with constant material parameters.

From the original IIM the idea of using a regular grid in spite of interfaces is kept. The corrections are added more similar to the earlier work [5]. Here, we concentrate on composite material problems, i.e. on the treatment of discontinuities in the equation coefficients. For the treatment of boundary conditions as jump conditions see [10].

We call points *regular* when the 9 point stencil of the standard central finite difference discrete Lamé operator Λ_h is not cut by the interface, all others *irregular points*. At regular points we can use the standard Λ_h. At irregular points, solution dependent *correction terms* that reduce the truncation error to first order are added.

$$\Lambda_h \mathcal{U} + \text{correction} = \mathcal{F} \ . \tag{5}$$

This turns out to be enough to keep the second order convergence of the solution, [8]. For example, in a situation like in Figure 1, the stencil of Λ_h at the point (x_i, y_j) is affected by four intersections of the interface with some grid line called *intersection points*, α_s, $s \in \{1, 2, 3, 4\}$.
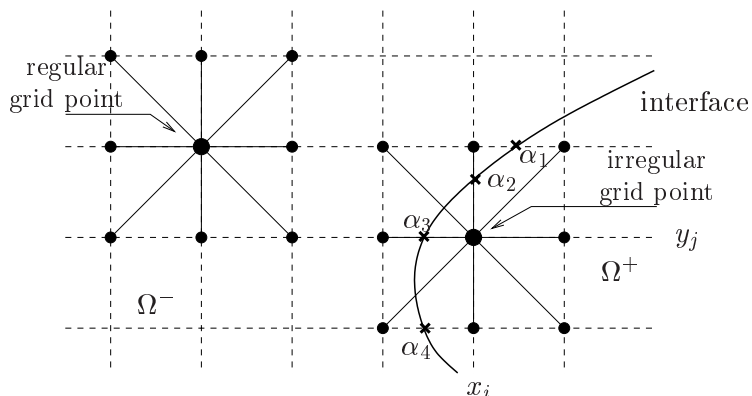
Figure 1: Regular and irregular grid points for the centered discrete Lamé operator Λ_h. The intersections of the interface with the grid lines mark the positions where the correction terms live.

The corrected finite difference approximation of the derivatives in the symmetric form in this situation is

$$\partial_{xx} u_{i,j} = \frac{1}{h^2} \left(u_{i-1,j} - 2u_{i,j} + u_{i+1,j} \right) + \frac{1}{h^2} \sum_{m=0}^{2} \frac{h_3^m}{m!} [\partial_x^m u]_{\alpha_3} + \mathcal{O}(h)$$

$$\partial_{yy} u_{i,j} = \frac{1}{h^2} \left(u_{i,j-1} - 2u_{i,j} + u_{i,j+1} \right) - \frac{1}{h^2} \sum_{m=0}^{2} \frac{h_2^m}{m!} [\partial_y^m u]_{\alpha_2} + \mathcal{O}(h)$$

$$\begin{aligned}
\partial_{xy}u_{i,j} \quad = \quad & \frac{1}{4h^2}\left(u_{i+1,j+1} - u_{i-1,j+1} - u_{i+1,j-1} + u_{i-1,j-1}\right) \\
& - \frac{1}{2h}\sum_{m=0}^{1}\frac{h_3^m}{m!}[\partial_x^m(\partial_y u)]_{\alpha_3} - \frac{1}{2h}\sum_{m=0}^{1}\frac{h_2^m}{m!}[\partial_y^m(\partial_x u)]_{\alpha_2} \\
& - \frac{1}{4h^2}\sum_{m=0}^{2}\frac{h_1^m}{m!}[\partial_x^m u]_{\alpha_1} + \frac{1}{4h^2}\sum_{m=0}^{2}\frac{h_4^m}{m!}[\partial_x^m u]_{\alpha_4} + \mathcal{O}(h),
\end{aligned}$$

where $h_1 = x_{i+1} - x_{\alpha_1}$, $h_2 = y_{j+1} - y_{\alpha_2}$, $h_3 = x_{i-1} - x_{\alpha_3}$, $h_4 = x_{i-1} - x_{\alpha_4}$ and (x_α, y_α) are the coordinates of the intersection point α.

In short, the correction terms can be always written in a form

$$\text{correction} = \sum_{s}\sum_{m=0}^{2}\psi_{m,s}[\partial^m u]_{\alpha_s} \tag{6}$$

with s counting the intersection points, α_s denoting the intersections of the interface with the grid lines and some coefficients $\psi_{m,s}$.

The essential distinction of the EJIIM is to *explicitly introduce the jumps as variables* in the discretized system. Additional equations are found expressing *interface conditions* as *jump conditions* that use only one-sided limits of derivatives at the interface. These limits are discretized by extrapolation of function values at the grid points on one side of the interface. We use the least squares fit for a 2-nd order polynomial. It can be briefly written as

$$[\partial^m u]_{\alpha_s} = \tilde{F}_s^u - \sum_{(i,j)\in\text{grid}}d_{s,(i,j,k)}^u U_{i,j,k} \, , \tag{7}$$

where $\tilde{F}^u$ denotes some vector of constants, containing, e.g., given jumps at the interface and $d_{s,(i,j,k)}^u$ are appropriately chosen coefficients multiplying the solution values $U_{i,j,k}$ that are non-zero only in a one-sided neighborhood of the interface point, see [10] for details.

The complete discretization can be written as

$$\begin{pmatrix} \mathbf{A} & \mathbf{\Psi} \\ \mathbf{D} & \mathbf{I} \end{pmatrix}\begin{pmatrix} \mathcal{U} \\ \mathcal{J} \end{pmatrix} = \begin{pmatrix} \mathcal{F} \\ \tilde{\mathcal{F}} \end{pmatrix} , \tag{8}$$

where $\mathbf{A}$ is the standard finite difference matrix, $\mathcal{F}$ is the discrete right hand side function, $\mathbf{\Psi}$ is the correction matrix (see (5) and (6)), $\mathcal{J}$ is the vector of the additional jump variables, $\mathbf{I}$ is the identity, $\mathbf{D}$ approximates the jump conditions (see Appendix) with components d^u and d^v and $\tilde{\mathcal{F}} := (\tilde{F}^u, \tilde{F}^v)^T$ comes from the extrapolation (7). Note that in this case, $\mathbf{A}$ has non-constant coefficients. Different from the Poisson equation case ([12]) and the single material elastostatic case ([10, 11]). This prohibits the use of an FFT based fast solver for the Schur-complement of the jumps, that requires constant coefficients.

For more details regarding (8) we refer to [10, 12]. The expressions for jumps in the case of composite materials in elasticity are given in the Appendix §A. For the homogeneous jump case they were first derived in [7].

We observed that iterative solvers applied to the full system (8) take a long time to converge or fail to converge at all, and use a direct solver instead. We conjecture that a fast iterative solver approach to (8) as is already available for the boundary value problem case will greatly alleviate these difficulties with iterative solvers and make the current approach also applicable for 3d problems.

Our method is very similar to the IIM by Yang and Li [13], where the IIM was applied to two dimensional composite material problems in linear elasticity.

Specifically, the similarities are

- Both methods use the standard central finite difference approximation at regular points.

- At irregular points, essentially the standard nine point stencil is used. The truncation error is reduced to first and higher order terms. This is known to be sufficient for second order convergence from numerical experiments. Significant progress towards a proof of this statement is made in [8]. Higher order corrections are easily incorporated but improve only the smoothness of the error [12].

- To reduce the truncation error at the irregular points, information about the known jumps, their arclength derivatives and jump in the right hand side of the equation is used.

On the other hand, there are significant differences:

- The idea of deriving the schemes is different. The IIM keeps the truncation error down by an underdetermined coefficients approach at the stencil points and adding a constant correction term. That is, the IIM computes a least-norm solution of an underdetermined system that arises from having more coefficients than equations that need to vanish. EJIIM uses the standard central finite difference approximation and adds correction terms, depending on the jumps in the function and its derivatives. These correction terms are found by least-squares solving an overdetermined system that arises from approximating more than 10 function values by a quadratic polynomial.

- EJIIM introduces explicitly the unknown jumps as additional variables in the system. To find additional, needed jump relations, extrapolation from one side is needed. Thus, approximation at the irregular point actually involves also all grid points which have been used in the extrapolation process. The stencil is larger than for the IIM.

- IIM uses optimization approach to guarantee a sign condition of the resulting matrices.

- Because of one-sided extrapolations near the interface, EJIIM leaves the freedom in selecting the extrapolation side if apriori information about the smoothness of the solution is available. Also, this one-sided extrapolation makes the EJIIM directly applicable to boundary value problems.

4 Examples

4.1 Convergence tests

Convergence analysis of the EJIIM has been completely done only for one dimensional problems [12]. For the two and three dimensional cases, only truncation error analysis is available. To prove convergence, one need to additionally show the boundedness of the inverse of the matrix in (8). This boundedness is believed to hold, and numerical tests have confirmed this fact for the discretization of Poisson-type operators (porous and composite materials) and for linear elasticity in the case of the porous media.

First we check the convergence with analytically known solutions. Second order finite difference schemes integrate polynomials up to second order exactly. This is also the case for EJIIM. We always have two possibilities in choosing the "-"–side for the formulas in the Appendix A. If the inclusion has been selected as "-" side, we call it *inner* EJIIM, otherwise *outer* EJIIM.

Example 1. This example is taken from Yang, Li and Li [13]. We recall the problem setup. The computational domain is $\Omega = (-1/2, 1/2)^2$ and the inclusion is an ellipsoid, parameterized by $x^2 + 4y^2 = 0.35^2$. The geometry is shown in Figure 2, left. Originally in [13], the Poisson's ratio ν and shear modulus μ are given. The Lamé coefficient is found by $\lambda = 2\mu\nu/(1 - 2\nu)$. This results in $\lambda^{incl} = 1.8642e + 6$ and $\mu^{incl} = 2e + 6$ in the inclusion. The material parameters of the matrix are $\lambda^{matr} = 1e + 6$ and $\mu^{matr} = 1.5e + 6$. Note that this is a so-called low-contrast problem, i.e. the properties of the two materials on the two sides of the interface are very similar. Also, it has the simplification that $[u_{xy}] = [v_{xy}] = 0$. The Dirichlét boundary conditions and the interface conditions are determined from the following exact solution:

$$u(x, y) = \begin{cases} xy + \sin(1 + x^2 + y^2) - 3x^2 + y^2 & \text{in} \quad \Omega^{matr} \\ xy + \sin(1 + x^2 + y^2) - 2x^2 + 5y^2 - 4 & \text{in} \quad \Omega^{incl} \end{cases}$$

$$v(x, y) = \begin{cases} \cos(1 + x^2 - y^2) + 5x^2y + x^2 - y^2 + 2 & \text{in} \quad \Omega^{matr} \\ \cos(1 + x^2 - y^2) + 5x^2y + 3x^2 + 7y^2 - 6 & \text{in} \quad \Omega^{incl} \end{cases}$$

The convergence results are shown in Table 1, where n denotes number of grid points in one direction. We see that we get results of practically the same quality as [13].

Example 2.

The interface is parametrized by $x = kr\cos\theta + x_c$, $y = kr\sin\theta + y_c$, $r = r_0 + 0.15\sin(w\theta)$. It has been adapted from [4]. We have taken $k = 0.55$, $(x_c, y_c) = (0.5, 0.5)$, $r_0 = 0.45$ and $w = 5$. The shape of the inclusion is shown in Figure 2, right. The material parameters have been taken to be the same as in the first example.

We consider also the more general situation, where the jump in the mixed derivatives is not zero, unlike Example 1. Also the other jumps in the second

7

Table 1: Grid refinement analysis for Example 1.

n	IIM ([13])	Ratio	EJIIM (inner)	Ratio	EJIIM (outer)	Ratio
$\|u^{numer} - u^{exact}\|_\infty$						
21	2.5749e-3	*	1.9014e-3	*	1.5861e-3	*
41	5.0891e-4	5.1	5.7598e-4	3.3	3.6251e-4	4.4
81	1.4667e-4	3.5	1.4091e-4	4.1	1.1071e-4	3.3
161	3.6265e-5	4.0	3.5606e-5	4.0	3.1528e-5	3.5
321	8.6890e-6	4.2	8.6865e-6	4.1	8.1558e-6	3.9
mean		4.2		3.9		3.8
$\|v^{numer} - v^{exact}\|_\infty$						
21	1.9612e-3	*	2.0271e-3	*	4.7272e-3	*
41	4.1027e-4	4.8	1.0370e-3	2.0	9.2140e-4	5.1
81	9.4880e-5	4.3	2.5161e-4	4.1	2.1958e-4	4.2
161	2.3726e-5	4.0	6.2382e-5	4.0	5.2726e-5	4.2
321	5.4118e-6	4.4	1.5366e-5	4.1	1.3286e-5	4.0
mean		4.4		3.5		4.4
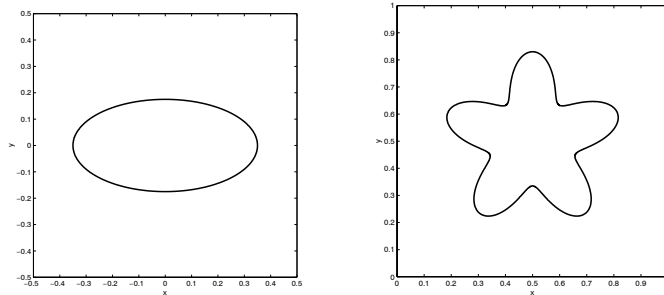
Figure 2: Shape of inclusions in Examples 1 (left) and 2 (right).

order derivatives are not constant. The exact solution is taken to be:

$$u(x,y) = \begin{cases} b_1(x - x_c) + \frac{b_2(x - x_c)}{r^2} & \text{in} \quad \Omega^{matr} \\ y^4 \sin(x^2 - y^2) & \text{in} \quad \Omega^{incl} \end{cases}$$

$$v(x,y) = \begin{cases} b_1(y - y_c) + \frac{b_2(y - y_c)}{r^2} & \text{in} \quad \Omega^{matr} \\ \exp(x) \cos(x^2 + y^2) & \text{in} \quad \Omega^{incl} \end{cases}$$

where $r^2 = (x - x_c)^2 + (y - y_c)^2$, with randomly selected constants $b_1 = 0.9501$, $b_2 = 0.2311$.

The convergence results are summarized in Table 2, where again n denotes the number of grid points in one direction. We see that second order convergence is achieved. Figures 4 and 5 show the error distribution with inner and outer EJIIM respectively. Typical for the Immersed Interface methods is a sharp resolution of the interface and no smearing of the solution as clearly seen in Figure 3.

8

Table 2: Grid refinement analysis for Example 2.

n	EJIIM (inner)	Ratio	EJIIM (outer)	Ratio
$\|u^{numer} - u^{exact}\|_\infty$				
21	6.0528e-3	*	1.1675e-1	*
41	1.2132e-3	5.0	1.4912e-2	7.8
81	3.7255e-4	3.3	6.6686e-3	2.2
161	8.2603e-5	4.5	2.1951e-3	3.0
321	1.5052e-5	5.5	5.6834e-4	3.9
mean		4.6		4.2
$\|v^{numer} - v^{exact}\|_\infty$				
21	8.3621e-3	*	1.8231e-1	*
41	2.5476e-3	3.3	1.9249e-2	9.5
81	5.6449e-4	4.5	6.0457e-3	3.2
161	1.9106e-4	3.0	2.8962e-3	2.1
321	3.3009e-5	5.8	7.0612e-4	4.1
mean		4.1		4.7
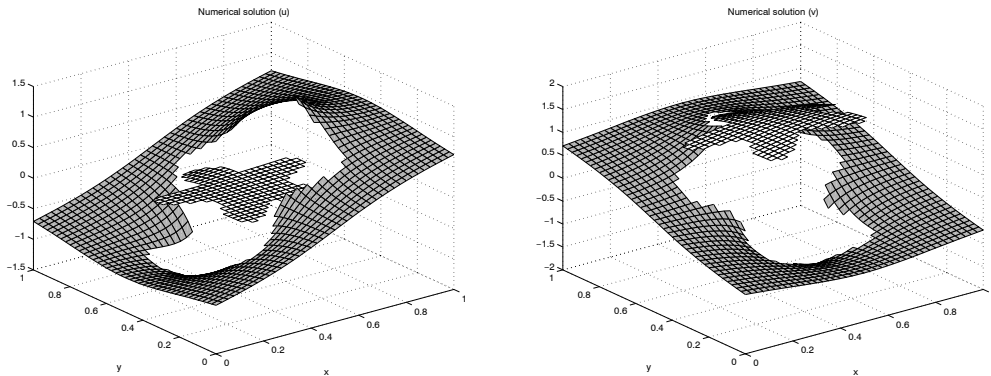
Figure 3: Numerical solution of Example 2 with outer EJIIM. Left: u, right: v.

Example 3.

We take the same setup as in the Example 2, but increase the contrast in the material parameters. The inclusion we take to be glass ($\lambda^{incl} \approx 54.66$, $\mu^{incl} \approx 25.72$) and the matrix is made of epoxy ($\lambda^{matr} \approx 0.95$, $\mu^{matr} \approx 1.43$).

The tesults are summarized in the Table 3, again n denotes the number of grid points in one direction.

We observe superconvergence. This means that the step sizes are not yet in the range where we really have second order convergence. The results are quantitavely worse than in the Example 2. However, is is notable that also in the case of high contrast the behavior is still stable and we do not get any oscillations at the interface.

9
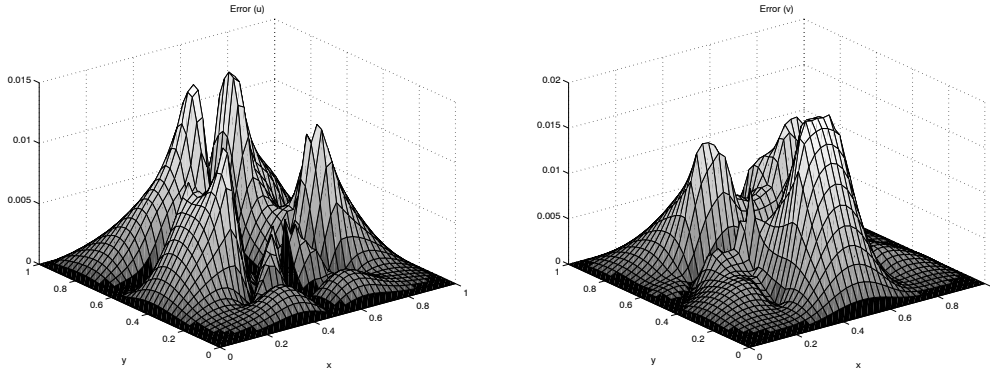
Figure 4: Absolute error in Example 2 with outer EJIIM. Left: u, right: v. $n = 41$.
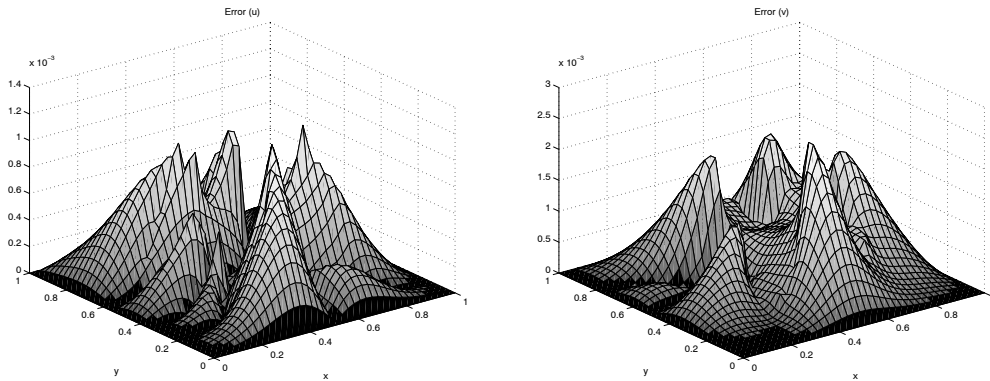
Figure 5: Absolute error in Example 2 with inner EJIIM. Left: u, right: v. $n = 41$.

5 Effective elastic moduli

The method presented here is based on the *strain energy conservation principle*, see e.g. [1], page 12: *the effective stiffness tensor is defined through the equality of the strain energy stored in the heterogeneous media to the strain energy stored in an equivalent homogeneous elastic media.*

For an overview about engineering methods to determine the effective elastic moduli we refer to [1]. A similar, more mathematical approach is homogenisation [2].

5.1 Algorithm

The total strain energy in the domain Ω is defined by

$$E = \frac{1}{2} \int_{\Omega} \varepsilon^{\top} C \varepsilon \,, \tag{9}$$

10

Table 3: Grid refinement analysis for Example 3.

n	EJIIM (inner)	Ratio	EJIIM (outer)	Ratio
$\|u^{numer} - u^{exact}\|_\infty$				
21	1.4883e+0	*	4.1930e-1	*
41	1.2821e-1	11.61	6.6424e-2	6.31
81	4.2403e-2	3.02	2.3808e-2	2.79
161	4.4471e-3	9.54	9.2901e-3	2.56
321	5.9293e-4	7.50	2.5384e-3	3.66
mean		7.92		3.83
$\|v^{numer} - v^{exact}\|_\infty$				
21	1.2755e+0	*	1.4036e+0	*
41	2.8115e-1	4.54	1.0188e-1	13.78
81	5.7841e-2	4.86	2.9580e-2	3.44
161	2.3631e-2	2.45	2.7734e-2	1.07
321	2.3300e-4	101.42	5.3972e-3	5.14
mean		28.32		5.86

where C is the stiffness tensor. In the iso-trope case C is given by

$$C = \begin{pmatrix} 2\mu + \lambda & \lambda & 0 \\ \lambda & 2\mu + \lambda & 0 \\ 0 & 0 & \mu \end{pmatrix} .$$

For general anisotropy we only know that C is symmetric and positive definite. With ε we denote the strains:

$$\varepsilon^\top = (\varepsilon_{xx}, \varepsilon_{yy}, 2\varepsilon_{xy}) = (\partial_x u, \partial_y v, \partial_x v + \partial_y u) . \tag{10}$$

In what follows, we will denote by E the strain energy computed using the local displacements in the heterogeneous media and with E_H—the strain energy in the equivalent homogeneous media. We will also use u_H and v_H to denote the displacements of the homogeneous media and C^H for the estimated effective (homogenized) stiffness tensor.

We can not find an effective C^H such that the strain energy is conserved for *all* possible displacements and every Ω. So we restrict ourselves to the space of constant strains in the homogeneous media and the representative volume element in our case is a rectangular domain. The following three basis vectors in the constant strain space are selected:

$$\varepsilon_H^1 = \begin{pmatrix} \beta \\ 0 \\ 0 \end{pmatrix} , \ \varepsilon_H^2 = \begin{pmatrix} 0 \\ \beta \\ 0 \end{pmatrix} , \ \varepsilon_H^3 = \begin{pmatrix} 0 \\ 0 \\ \beta \end{pmatrix} , \tag{11}$$

11

where $0 < \beta \ll 1$ to be in the regime of linear elasticity. Due to the fact that

$$
\begin{aligned}
E(\alpha\varepsilon) &= \alpha^2 E(\varepsilon) \\
E(\varepsilon^1 + \varepsilon^2) &= E(\varepsilon^1) + E(\varepsilon^2) + \int_\Omega (\varepsilon^1)^\top C \varepsilon^2
\end{aligned}
\tag{12}
$$

three basis strain vectors suffice to guarantee the energy conservation for all constant strains in homogeneous media.

Three displacements which generate the base strains in (11) are

$$
\begin{cases} u_H^1 = \beta(x - m_x) \\ v_H^1 = 0 \end{cases} ,\quad
\begin{cases} u_H^2 = 0 \\ v_H^2 = \beta(y - m_y) \end{cases} ,\quad
\begin{cases} u_H^3 = \beta(y - m_y) \\ v_H^3 = 0 \end{cases} ,
$$

where $\Omega = (a_x, b_x) \times (a_y, b_y)$ and $m_x = (a_x + b_x)/2$, $m_y = (a_y + b_y)/2$. The set of experiments is not unique and illustrated in Figure 6.
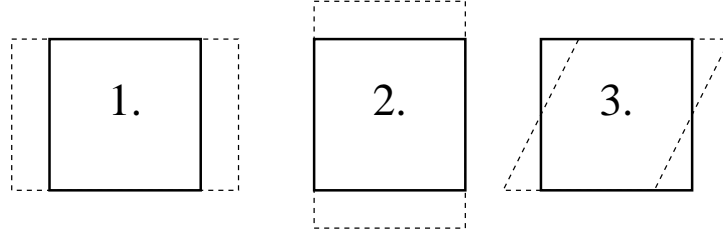
Figure 6: Three experiments for determining the effective elastic moduli.

With this we can now state the algorithm.

1. At first we derive the energies using (9) for all three experiments assuming that the material is homogeneous with unknown stiffness tensor C_H. By E_H^{ii} we denote the energy in the i-th experiment. As C^H is constant, we get that

$$
E_H^{ii} = \frac{1}{2}\mathrm{vol}(\Omega)(\varepsilon_H^i)^\top C^H \varepsilon_H^i = \frac{1}{2}\beta^2 C_{ii}^H \ ,\ i \in \{1,\, 2,\, 3\}\ .
$$

We need to compute also the mixed term in (12), we denote it by E_H^{ij}. Here it is

$$
E_H^{ij} = \frac{1}{2}\mathrm{vol}(\Omega)(\varepsilon_H^i)^\top C^H \varepsilon_H^j = \frac{1}{2}\beta^2 C_{ij}^H \ ,\ i,j \in \{1,\, 2,\, 3\}\ .
$$

2. The second step is to perform three numerical experiments. On $\partial\Omega$ we specify Dirichlet boundary conditions. Concretely, $\mathbf{u} = \mathbf{u}_H^i$, $i \in \{1,\, 2,\, 3\}$. In each experiment we calculate the entries of the strain vector (10).

3. Finall, we use the calculated strains to compute E^{ij}, $i \in \{1,\, 2,\, 3\}$ using (9) and the mixed term in (12). We set $E^{ij} = E_H^{ij}$ and thus get entries of the homogenised stiffness tensor C^H using formulas obtained in the first step.

5.2 Example

We take a composite material consisting of epoxy matrix and glass inclusions, the material parameters are taken from Example 3. The shape of the inclusion is ellipsoidal, characterised by

$$\frac{(x - x_c)^2}{a^2} + \frac{(y - y_c)^2}{b^2} \leq 1 \,.$$

We change the axis in x-direction, a, from 0.2 to 0.45. The second radius, b, is selected in such way that the area of the ellipse is always 0.3. The domain is $(-0.5, 0.5)^2$ and $(x_c, y_c) = (0, 0)$. All calculations are performed using 120 grid points in each direction for the grid.
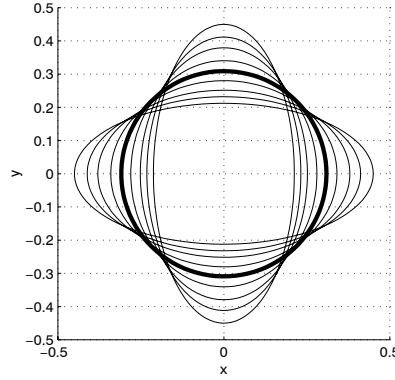
Figure 7: Geometries in the effective elastic moduli calculations.

As the inclusion is symmetric with respect to the x and y axis, we expect at least ortho-trope symmetry. In the result summary in figure 8 we see that indeed the entries C_{13}^H and C_{23}^H are negligible, identifying the orthotropy. Because of this we can proceed one more step and extract engineering constants. For ortho-trope materials, the stiffness tensor is given by

$$C = \frac{1}{1 - \nu_{12}\nu_{21}} \begin{pmatrix} K_1 & \nu_{21}K_1 & 0 \\ \nu_{12}K_2 & K_2 & 0 \\ 0 & 0 & \mu(1 - \nu_{12}\nu_{21}) \end{pmatrix} \,,$$

where K_i is the Young's moduli in the $i - th$ direction, μ is the shear modulus and ν_{ij} is the Poisson's ratio for transverse strain in the j-th direction when the material is stressed in the i-th direction. Using this form of C, we find that

$$K_1 = C_{11} - \frac{C_{12}^2}{C_{22}} \,, \;\; K_2 = C_{22} - \frac{C_{21}^2}{C_{11}}$$

$$\nu_{12} = \frac{C_{21}}{C_{22}} \,, \;\; \nu_{21} = \frac{C_{12}}{C_{11}} \,, \;\; \mu = C_{33} \,.$$

The effective parameters are shown in figure 9. Note that all curves are symmetric about the value $\bar{a} = \sqrt{0.3/\pi}$ because with the axes pair (a, b) we have
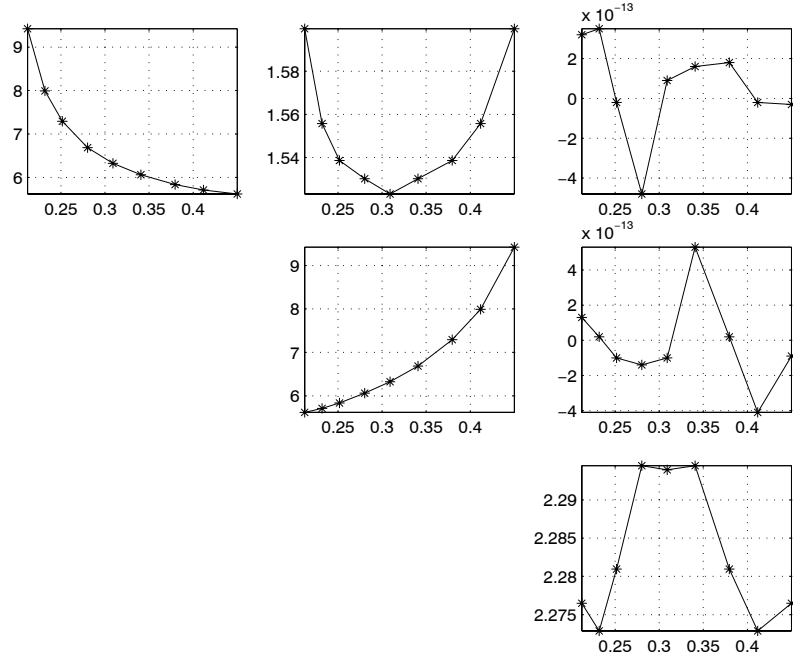
Figure 8: Numerically calculated entries of the effective stiffness tensor. On the x-axis we mark the length a of the ellipse in the x-direction.
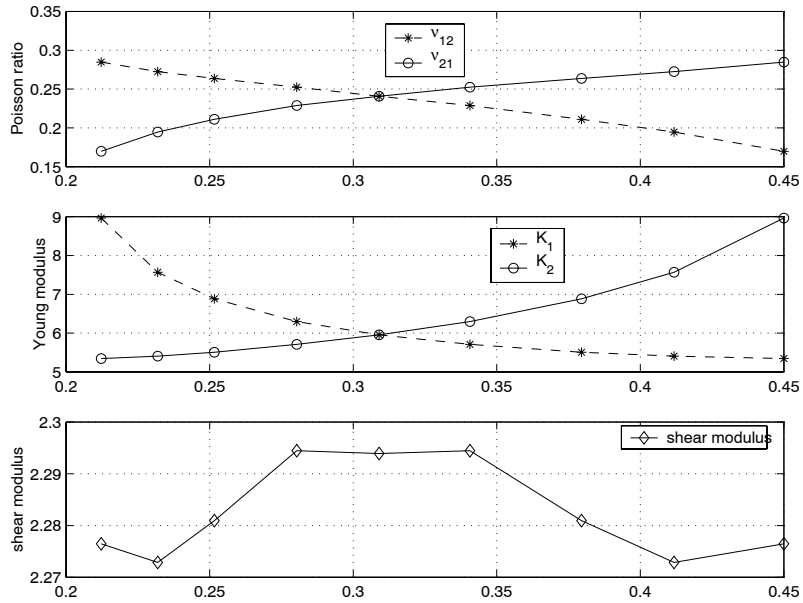
Figure 9: The effective engineering constants corresponding to the stiffness tensor in figure 8. On the x-axis we mark the length a of the ellipse in the x-direction.

also included the pair (b, a). The point $\bar{a}$ corresponds to the circular inclusion (thick line in figure 7).

For virtual material design, the dependence of these effective parameters on the shape and position of the inclusion as well as on the contrast of the individual properties is highly significant. To design a material with given effective properties, one needs to compute the effective properties for many trial geometries rather quickly. This will be possible with the current methodology even in three space dimensions once the final building block, a fast iterative solver for composite elastic materials, is found.

6   Conclusions

We have applied the Explicit Jump Immersed Interface Method (EJIIM) to composite material problems in planar linear elasticity. The EJIIM is a finite difference method, where the standard central finite differences are corrected by jump-dependent correction terms in the case when the standard stencil is affected by the interface. The essential distinction of the EJIIM is to *explicitly introduce the jumps as variables* in the discretized system. Additional equations are found expressing *interface conditions* as *jump conditions* that use only one sided derivatives. The one sided limits of derivatives on the interface are discretized by extrapolation of function values at the grid points on one side of the interface. From the point of view of the EJIIM discretization, singular source term problems, boundary value problems and discontinuous coefficient problems differ only by the expressions used in the first step.

The EJIIM approach leads to large scale and not always well-conditioned linear systems of equations. Solving these equations is by no means trivial, and unfortunately the FFT-based techniques that are available for the Poisson-type equations for compoiste problems and boundary value problems and for linear elasticity in the boundary value case could not yet be transferred to the composite material elasticity case. Thus, good preconditioning and solution techniques are still open questions.

In this paper we have given the necessary formulas for jumps in composite material problems of two-dimensional linear elasticity and presented numerical results that confirm the second order convergence of the displacements in the maximum norm.

Convergence of the numerical method with respect to the contrast is worth separate study, as contrast may dominate over the errors done in approximation. Example 3 shows that this is relevant also in our situation. It would be necessary to understand contrast in which coefficients really determine the numerical behavior of the scheme.

Finally we have given an idea how virtual material design of effective elastic moduli may be executed using the EJIIM.

A   Jump conditions for discontinous coefficients

The expressions for jumps are found first in local coordinates at the point where the interface intersects the grid. Then a coordinate transformation yields the jump conditions in (x, y) coordinates. In [7] the formulas for a simpler case, with continuous solution and normal stresses, were already reported. Here we extend the method to the general case of inhomogeneous jumps.

A.1   Local coordinates

At a point P lying on the interface we introduce the local coordinates $(\mathbf{n}, \mathbf{t})$ with $\mathbf{n}$ being the normal and $\mathbf{t}$ tangential vector in such a way that they form a right hand system Figure 10.
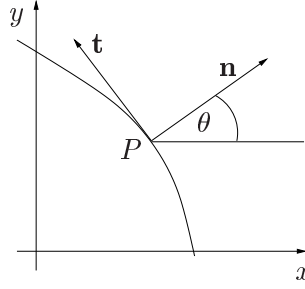
Figure 10: Local coordinates at the interface.

Then displacements in directions $\mathbf{n}$ and $\mathbf{t}$ are ξ and η respectively:

$$\xi = \mathbf{u} \cdot \mathbf{n} \quad \text{and} \quad \eta = \mathbf{u} \cdot \mathbf{t} \,.$$

The stress tensor is expressed in the new coordinates:

$$\tilde{\boldsymbol{\sigma}} := \begin{pmatrix} \sigma_{nn} & \sigma_{nt} \\ \sigma_{nt} & \sigma_{tt} \end{pmatrix} = \mu \begin{pmatrix} 2\partial_n\xi & \partial_t\xi + \partial_n\eta \\ \partial_t\xi + \partial_n\eta & 2\partial_t\eta \end{pmatrix} + \lambda \begin{pmatrix} \Theta & 0 \\ 0 & \Theta \end{pmatrix} \tag{13}$$

with $\Theta = \partial_n\xi + \partial_t\eta$. The notations ∂_n and ∂_t mean directional derivatives in $\mathbf{n}$ and $\mathbf{t}$ directions respectively.

The normal in the local coordinates is simply $(1, 0)^T$ and thus we get from the interface conditions (3) and (4) by using (13)

$$\begin{align} [\xi] &= \bar{\mathbf{u}} \cdot \mathbf{n} \tag{14} \\ [\eta] &= \bar{\mathbf{u}} \cdot \mathbf{t} \tag{15} \\ [(2\mu + \lambda)\partial_n\xi + \lambda\partial_t\eta] &= \mathbf{g} \cdot \mathbf{n} \tag{16} \\ [\mu (\partial_t\xi + \partial_n\eta)] &= \mathbf{g} \cdot \mathbf{t}. \tag{17} \end{align}$$

A.2   Jumps in Cartesian coordinates

In principle, we can derive jumps in the derivatives of arbitrary order by noting that $\mathrm{d}_l[g(P)] = [\mathrm{d}_l g(P)]$ at some point P, with arclength parameter l.

We need jumps in derivatives in the coordinate directions. Let $\theta = \theta(l)$ as shown in Figure 10. To simplify notations we introduce $\mathsf{s} := \sin(\theta(l))$ and $\mathsf{c} := \cos(\theta(l))$. Then $\mathbf{n} = (\mathsf{c}, \mathsf{s})$ and $\mathbf{t} = (-\mathsf{s}, \mathsf{c})$.

The two **jumps in the zeroth order derivatives** are given by (3),

$$
\begin{aligned}
{}[u] &= \bar{u}, \\
{}[v] &= \bar{v}.
\end{aligned}
$$

Four jumps **in the first order derivatives** need to be determined. Stress continuity (16, 17) gives immediately two relations, and two more relations we obtain by continuity of arclength derivatives of $\bar{\mathbf{u}}$. After some calculations and use of the fact that

$$
[\gamma p] = \gamma^+ [p] + [\gamma] p^-
$$

for some function p and coefficient γ we get the jumps in first order derivatives as solution of a system

$$
\mathbf{M} \mathcal{J}^1(P) = G
$$

with $\mathcal{J}^1(P) := [(u_x, u_y, v_x, v_y)^T]_P$ and

$$
\mathbf{M} = \begin{pmatrix}
\beta^+ \mathsf{c}^2 + \lambda^+ \mathsf{s}^2 & 2\mu^+ \mathsf{s}\mathsf{c} & 2\mu^+ \mathsf{s}\mathsf{c} & \beta^+ \mathsf{s}^2 + \lambda^+ \mathsf{c}^2 \\
-2\mu^+ \mathsf{s}\mathsf{c} & \mu^+ (\mathsf{c}^2 - \mathsf{s}^2) & \mu^+ (\mathsf{c}^2 - \mathsf{s}^2) & 2\mu^+ \mathsf{s}\mathsf{c} \\
-s & c & 0 & 0 \\
0 & 0 & -\mathsf{s} & \mathsf{c}
\end{pmatrix}
$$

and $G = (G_1, G_2, \mathrm{d}_l \bar{u}, \mathrm{d}_l \bar{v})^T$ with

$$
\begin{aligned}
G_1 &= \mathbf{g} \cdot \mathbf{n} - [\beta](\mathsf{c}^2 u_x^- + \mathsf{s}\mathsf{c}(u_y^- + v_x^-) + \mathsf{s}^2 v_y^-) \\
&\quad - [\lambda](\mathsf{s}^2 u_x^- - \mathsf{s}\mathsf{c}(u_y^- + v_x^-) + \mathsf{c}^2 v_y^-) \\
G_2 &= \mathbf{g} \cdot \mathbf{t} - [\mu](-2\mathsf{s}\mathsf{c}u_x^- + (\mathsf{c}^2 - \mathsf{s}^2)(u_y^- + v_x^-) + 2\mathsf{s}\mathsf{c}v_y^-)
\end{aligned}
$$

Now six jumps **in the second order derivatives** need to be determined. Two relations are obtained by taking the second order arclength derivatives of the displacements, two relations can be gotten from the equation (1) itself and for the two missing ones we take the arclength derivatives of (16, 17):

$$
\begin{aligned}
{}[\mathrm{d}_{ll} u] &= \mathrm{d}_{ll} \bar{u} \\
{}[\mathrm{d}_{ll} v] &= \mathrm{d}_{ll} \bar{v} \\
{}[\mu \Delta u + (\mu + \lambda)(u_{xx} + v_{xy})] &= [f_1] \\
{}[\mu \Delta v + (\mu + \lambda)(u_{xy} + v_{yy})] &= [f_2] \\
{}[\mathrm{d}_l (\mu (\partial_t \xi + \partial_n \eta))] &= \mathrm{d}_l (\mathbf{g} \cdot \mathbf{t}) \\
{}[\mathrm{d}_l (\beta \partial_n \xi + \lambda \partial_t \eta)] &= \mathrm{d}_l (\mathbf{g} \cdot \mathbf{n}).
\end{aligned}
\tag{18}
$$

After rather lengthy calculations we get jumps in the second order derivatives at the point P as the solution of the following system:

$$\mathtt{M}\mathcal{J}^2(P) = \mathtt{G} \tag{19}$$

with $\mathcal{J}^2(P) = [(u_{xx}, u_{xy}, u_{yy}, v_{xx}, v_{xy}, v_{yy})^T]_P$ and

$$
\mathtt{M} = \begin{pmatrix}
\mathtt{s}^2 & -2\mathtt{s}\mathtt{c} & \mathtt{c}^2 & 0 & 0 & 0 \\
0 & 0 & 0 & \mathtt{s}^2 & -2\mathtt{s}\mathtt{c} & \mathtt{c}^2 \\
\beta^+ & 0 & \mu^+ & 0 & \mu^+ + \lambda^+ & 0 \\
0 & \mu^+ + \lambda^+ & 0 & \mu^+ & 0 & \beta^+ \\
\mathtt{m}_{51} & \mathtt{m}_{52} & \mathtt{m}_{53} & \mathtt{m}_{54} & \mathtt{m}_{55} & \mathtt{m}_{56} \\
\mathtt{m}_{61} & \mathtt{m}_{62} & \mathtt{m}_{63} & \mathtt{m}_{64} & \mathtt{m}_{65} & \mathtt{m}_{66}
\end{pmatrix},
$$

where

$$
\begin{aligned}
\mathtt{m}_{51} &= 2\mu^+ \mathtt{s}^2\mathtt{c} & \mathtt{m}_{61} &= -\beta^+\mathtt{s}\mathtt{c}^2 - \lambda^+\mathtt{s}^3 \\
\mathtt{m}_{52} &= \mu^+\left(\mathtt{s}^3 - 3\mathtt{s}\mathtt{c}^2\right) & \mathtt{m}_{62} &= \beta^+\left(\mathtt{c}^3 - \mathtt{s}^2\mathtt{c}\right) + 2\lambda^+\mathtt{s}^2\mathtt{c} \\
\mathtt{m}_{53} &= \mu^+\left(\mathtt{c}^3 - \mathtt{s}^2\mathtt{c}\right) & \mathtt{m}_{63} &= \left(\beta^+ - \lambda^+\right)\mathtt{s}\mathtt{c}^2 \\
\mathtt{m}_{54} &= \mu^+\left(\mathtt{s}^3 - \mathtt{s}\mathtt{c}^2\right) & \mathtt{m}_{64} &= \left(\lambda^+ - \beta^+\right)\mathtt{s}^2\mathtt{c} \\
\mathtt{m}_{55} &= \mu^+\left(\mathtt{c}^3 - 3\mathtt{s}^2\mathtt{c}\right) & \mathtt{m}_{65} &= \beta^+\left(\mathtt{s}\mathtt{c}^2 - \mathtt{s}^3\right) - 2\lambda^+\mathtt{s}\mathtt{c}^2 \\
\mathtt{m}_{56} &= 2\mu^+\mathtt{s}\mathtt{c}^2 & \mathtt{m}_{66} &= \beta^+\mathtt{s}^2\mathtt{c} + \lambda^+\mathtt{c}^3 .
\end{aligned}
$$

The entries of $\mathtt{G}$ are given by:

$$
\begin{aligned}
\mathtt{G}_1 &= \left([u_x]\,\mathtt{c} + [u_y]\,\mathtt{s}\right) \mathrm{d}_l\theta + \mathrm{d}_{ll}\bar{u} \\
\mathtt{G}_2 &= \left([v_x]\,\mathtt{c} + [v_y]\,\mathtt{s}\right) \mathrm{d}_l\theta + \mathrm{d}_{ll}\bar{v} \\
\mathtt{G}_3 &= [f_1] - \left([\mu]\Delta u^- + ([\mu] + [\lambda])\left(u_{xx}^- + v_{xy}^-\right)\right) \\
\mathtt{G}_4 &= [f_2] - \left([\mu]\Delta v^- + ([\mu] + [\lambda])\left(u_{xy}^- + v_{yy}^-\right)\right) \\
\mathtt{G}_5 &= \mathrm{d}_l(\mathbf{g}\cdot\mathbf{t}) \\
&\quad + 2\mu^+\left(\left(\mathtt{c}^2 - \mathtt{s}^2\right)([u_x] - [v_y]) + 2\mathtt{s}\mathtt{c}\left([v_x] + [u_y]\right)\right) \mathrm{d}_l\theta \\
&\quad + 2[\mu]\left(\left(\mathtt{c}^2 - \mathtt{s}^2\right)\left(u_x^- - v_y^-\right) + 2\mathtt{s}\mathtt{c}\left(v_x^- + u_y^-\right)\right) \mathrm{d}_l\theta \\
&\quad - [\mu]\left(2\mathtt{s}^2\mathtt{c}u_{xx}^- + \left(\mathtt{s}^3 - 3\mathtt{s}\mathtt{c}^2\right)u_{xy}^- + \left(\mathtt{c}^3 - \mathtt{s}^2\mathtt{c}\right)u_{yy}^- \right. \\
&\quad \left. + \left(\mathtt{s}^3 - \mathtt{s}\mathtt{c}^2\right)v_{xx}^- + \left(\mathtt{c}^3 - 3\mathtt{s}^2\mathtt{c}\right)v_{xy}^- + 2\mathtt{s}\mathtt{c}^2 v_{yy}^-\right) \\
\mathtt{G}_6 &= \mathrm{d}_l(\mathbf{g}\cdot\mathbf{n}) \\
&\quad + \left(\beta^+ - \lambda^+\right)\left(2\mathtt{s}\mathtt{c}([u_x] - [v_y]) + \left(\mathtt{s}^2 - \mathtt{c}^2\right)([u_y] + [v_x])\right) \mathrm{d}_l\theta \\
&\quad + ([\beta] - [\lambda])\left(2\mathtt{s}\mathtt{c}\left(u_x^- - v_y^-\right) + \left(\mathtt{s}^2 - \mathtt{c}^2\right)\left(u_y^- + v_x^-\right)\right) \mathrm{d}_l\theta \\
&\quad + [\beta]\left(\mathtt{s}\mathtt{c}^2 u_{xx}^- + \left(\mathtt{s}^2\mathtt{c} - \mathtt{c}^3\right)u_{xy}^- - \mathtt{s}\mathtt{c}^2 u_{yy}^- \right. \\
&\quad \left. + \mathtt{s}^2\mathtt{c}v_{xx}^- + \left(\mathtt{s}^3 - \mathtt{s}\mathtt{c}^2\right)v_{xy}^- - \mathtt{s}^2\mathtt{c}v_{yy}^-\right) \\
&\quad + [\lambda]\left(\mathtt{s}^3 u_{xx}^- - 2\mathtt{s}^2\mathtt{c}u_{xy}^- + \mathtt{s}\mathtt{c}^2 u_{yy}^- - \mathtt{s}^2\mathtt{c}v_{xx}^- + 2\mathtt{s}\mathtt{c}^2 v_{xy}^- - \mathtt{c}^3 v_{yy}^-\right) .
\end{aligned}
$$

These systems can be solved analytically for $\mathcal{J}^2(P)$ by any computer algebraic programm, e.g., *Maple*. To make use of $\mathcal{J}^1(P)$ and $\mathcal{J}^2(P)$, one-sided extrapolation that approximates $u^-, v^-, u_x^-, u_y^-, v_x^-, v_y^-, u_{xx}^- \ldots, v_{yy}^-$ are discretized in the operator D as in [10].

We include the three second order jump conditions for the horizontal displacement. Those for the vertical displacement are similar. Again, Maple was essential to find these formulas and to generate the codes for our numerical examples.

$$\mu(2\mu + \lambda)[u_{xx}] =$$
$$\left(8\,\mu^2\,\mathsf{c}^5 - 6\,\mu^2\,\mathsf{c} + 12\,\mathsf{c}^3\,\mu^2 - 8\,\mu\,\mathsf{c}^5\,\lambda - 3\,\mu\,\lambda\,\mathsf{c} + 10\,\mu\,\mathsf{c}^3\,\lambda\right)[u_x]\,\mathrm{d}_l\theta$$
$$+\left(2\,\mu^2\,\mathsf{s} + \mu\,\mathsf{s}\,\lambda + 4\,\mu^2\,\mathsf{s}\,\mathsf{c}^2 + 2\,\mu\,\mathsf{s}\,\mathsf{c}^2\,\lambda - 8\,\mu^2\,\mathsf{s}\,\mathsf{c}^4 - 8\,\mu\,\mathsf{c}^4\,\lambda\,\mathsf{s}\right)[u_y]\,\mathrm{d}_l\theta$$
$$+\left(8\,\mu\,\mathsf{s}\,\mathsf{c}^2\,\lambda - 8\,\mu\,\mathsf{c}^4\,\lambda\,\mathsf{s} - 8\,\mu^2\,\mathsf{s}\,\mathsf{c}^4 + 10\,\mu^2\,\mathsf{s}\,\mathsf{c}^2\right)[v_x]\,\mathrm{d}_l\theta$$
$$+\left(8\,\mu^2\,\mathsf{c}^5 - 10\,\mathsf{c}^3\,\mu^2 + 4\,\mu^2\,\mathsf{c} - 8\,\mu\,\mathsf{c}^3\,\lambda + 2\,\mu\,\lambda\,\mathsf{c} + 8\,\mu\,\mathsf{c}^5\,\lambda\right)[v_y]\,\mathrm{d}_l\theta$$
$$-\left(\left(8\,\mu\,\mathsf{c}^4 + 6\,\lambda - 14\,\mathsf{c}^2\,\lambda - 18\,\mu\,\mathsf{c}^2 + 8\,\mathsf{c}^4\,\lambda + 12\,\mu\right)[\mu] + \left(-2\,\mu\,\mathsf{c}^2\,[\lambda] + 3\,\mu\,[\lambda]\right)[\lambda]\right)\mathsf{c}^2\,u_{xx}^-$$
$$+\left(8\,\mathsf{c}^6\,\lambda + \mathsf{c}^2\,\lambda - 8\,\mathsf{c}^4\,\lambda - 10\,\mu\,\mathsf{c}^4 + 8\,\mu\,\mathsf{c}^6 + 2\,\mu\,\mathsf{c}^2\right)[\mu]\,u_{yy}^-$$
$$-\left(\left(2\,\mathsf{s}\,\mathsf{c}\,\lambda - 20\,\mu\,\mathsf{s}\,\mathsf{c}^3 + 16\,\mu\,\mathsf{s}\,\mathsf{c}^5 - 14\,\mathsf{s}\,\mathsf{c}^3\,\lambda + 4\,\mu\,\mathsf{s}\,\mathsf{c} + 16\,\mathsf{s}\,\mathsf{c}^5\,\lambda\right)[\mu] - 2\,\mu\,\mathsf{s}\,\mathsf{c}^3\,[\lambda]\right)u_{xy}^-$$
$$+\left(10\,\mathsf{s}\,\mathsf{c}^3\,\lambda + 12\,\mu\,\mathsf{s}\,\mathsf{c}^3 - 8\,\mu\,\mathsf{s}\,\mathsf{c}^5 - 8\,\mathsf{s}\,\mathsf{c}^5\,\lambda - 2\,\mathsf{s}\,\mathsf{c}\,\lambda - 4\,\mu\,\mathsf{s}\,\mathsf{c}\right)[\mu]\,v_{xx}^-$$
$$-\left(4\,\mu\,\mathsf{s}\,\mathsf{c}^3\,[\mu] + 4\,\mathsf{s}\,\mathsf{c}^3\,\lambda\,[\mu] - 8\,\mu\,\mathsf{s}\,\mathsf{c}^5\,[\mu] - 8\,\mathsf{s}\,\mathsf{c}^5\,\lambda\,[\mu] - 2\,\mu\,\mathsf{s}\,\mathsf{c}^3\,[\lambda]\right)v_{yy}^-$$
$$+\left(\left(16\,\mathsf{c}^6\,\lambda - 22\,\mathsf{c}^4\,\lambda + 7\,\mathsf{c}^2\,\lambda - 24\,\mu\,\mathsf{c}^4 + 16\,\mu\,\mathsf{c}^6 + 8\,\mu\,\mathsf{c}^2\right)[\mu] + \left(2\,\mu\,\mathsf{c}^4\,[\lambda] - 3\,\mu\,\mathsf{c}^2\,[\lambda]\right)[\lambda]\right)v_{xy}^-$$
$$-3\,\mathsf{c}^3\,\mathrm{d}_l(\mathbf{g}\cdot\mathbf{t})\,\lambda + 16\,[\mu]\,\mathrm{d}_l\theta\,v_y^-\,\mathsf{c}^5\,\lambda - 16\,\mu\,\mathsf{s}\,[\mu]\,\mathrm{d}_l\theta\,\mathsf{c}^4\,u_y^- - 16\,\mu\,[\mu]\,\mathrm{d}_l\theta\,u_x^-\,\mathsf{c}^5$$
$$+16\,\mu\,[\mu]\,\mathrm{d}_l\theta\,v_y^-\,\mathsf{c}^5 - 16\,\mu\,\mathsf{s}\,[\mu]\,\mathrm{d}_l\theta\,\mathsf{c}^4\,v_x^- + 8\,\mu\,\mathsf{s}\,\mathsf{c}^3\,\mathrm{d}_{ll}\bar{v}\,\lambda - 5\,\mu\,\mathsf{c}^3\,\mathrm{d}_l(\mathbf{g}\cdot\mathbf{t})$$
$$+\mu\,\lambda\,\mathrm{d}_{ll}\bar{u} + 8\,\mu^2\,\mathsf{s}\,\mathsf{c}^3\,\mathrm{d}_{ll}\bar{v} - 16\,[\mu]\,\mathrm{d}_l\theta\,u_x^-\,\mathsf{c}^5\,\lambda - 16\,\mathsf{s}\,[\mu]\,\mathrm{d}_l\theta\,\mathsf{c}^4\,u_y^-\,\lambda$$
$$-16\mathsf{s}\,[\mu]\,\mathrm{d}_l\theta\,\mathsf{c}^4\,v_x^-\,\lambda + 8\,\mu\,\mathsf{c}^4\,\lambda\,\mathrm{d}_{ll}\bar{u} - \mu\,\mathsf{s}\,\mathsf{c}^2\,\mathrm{d}_l(\mathbf{g}\cdot\mathbf{n}) + \mathsf{s}\,\mathsf{c}^2\,\mathrm{d}_l(\mathbf{g}\cdot\mathbf{n})\,\lambda + 2\,\mu^2\,\mathrm{d}_{ll}\bar{u}$$
$$-8\,\mu\,\mathsf{c}^2\,\lambda\,\mathrm{d}_{ll}\bar{u} - \mu\,\mathsf{s}\,\mathsf{c}^3\,f_2 - 4\,\mu^2\,\mathsf{s}\,\mathsf{c}\,\mathrm{d}_{ll}\bar{v} - \mathsf{s}\,\mathsf{c}^3\,\lambda\,f_2 - 4\,\mathsf{c}\,[\mu]\,\mathrm{d}_l\theta\,u_x^-\,\lambda + 4\,\mathsf{c}\,[\mu]\,\mathrm{d}_l\theta\,v_y^-\,\lambda$$
$$-18\,[\mu]\,\mathrm{d}_l\theta\,v_y^-\,\mathsf{c}^3\,\lambda + 18\,[\mu]\,\mathrm{d}_l\theta\,u_x^-\,\mathsf{c}^3\,\lambda + 22\,\mu\,[\mu]\,\mathrm{d}_l\theta\,u_x^-\,\mathsf{c}^3 - 22\,\mu\,[\mu]\,\mathrm{d}_l\theta\,v_y^-\,\mathsf{c}^3 + 8\,\mu\,\mathsf{c}\,[\mu]\,\mathrm{d}_l\theta\,v_y^-$$
$$-8\,\mu\,\mathsf{c}\,[\mu]\,\mathrm{d}_l\theta\,u_x^- + 10\,\mathsf{s}\,[\mu]\,\mathrm{d}_l\theta\,\mathsf{c}^2\,u_y^-\,\lambda + 10\,\mathsf{s}\,[\mu]\,\mathrm{d}_l\theta\,\mathsf{c}^2\,v_x^-\,\lambda - 2\,\mu\,\mathsf{s}\,\mathsf{c}\,\mathrm{d}_{ll}\bar{v}\,\lambda + 14\,\mu\,\mathsf{s}\,[\mu]\,\mathrm{d}_l\theta\,\mathsf{c}^2\,u_y^-$$
$$+14\,\mu\,\mathsf{s}\,[\mu]\,\mathrm{d}_l\theta\,\mathsf{c}^2\,v_x^- + 2\,\mu\,\mathsf{c}^2\,f_1 - \mathsf{c}^2\,f_1\,\lambda - \mathsf{c}^4\,f_1\,\lambda + 2\,\mathsf{c}\,\lambda\,\mathrm{d}_l(\mathbf{g}\cdot\mathbf{t})$$
$$+4\,\mu\,\mathsf{c}\,\mathrm{d}_l(\mathbf{g}\cdot\mathbf{t}) - \mu\,\mathsf{c}^4\,f_1 - 10\,\mu^2\,\mathrm{d}_{ll}\bar{u}\,\mathsf{c}^2 + 8\,\mathsf{c}^4\,\mu^2\,\mathrm{d}_{ll}\bar{u}$$

$\mu(2\mu + \lambda)[u_{xy}] =$

$\left(8\,\mu\,\mathsf{s}\,\mathsf{c}^2\,\lambda + 10\,\mu^2\,\mathsf{s}\,\mathsf{c}^2 - 2\,\mu\,\mathsf{s}\,\lambda - 4\,\mu^2\,\mathsf{s} - 8\,\mu\,\mathsf{c}^4\,\lambda\,\mathsf{s} - 8\,\mu^2\,\mathsf{s}\,\mathsf{c}^4\right)[u_x]\,\mathrm{d}_l\theta$

$\quad - \left(10\,\mathsf{c}^3\,\mu^2 + 8\,\mu\,\mathsf{c}^3\,\lambda - 8\,\mu\,\mathsf{c}^5\,\lambda - 8\,\mu^2\,\mathsf{c}^5\right)[u_y]\,\mathrm{d}_l\theta$

$\quad - \left(16\,\mathsf{c}^3\,\mu^2 + 14\,\mu\,\mathsf{c}^3\,\lambda - 6\,\mu^2\,\mathsf{c} - 5\,\mu\,\lambda\,\mathsf{c} - 8\,\mu\,\mathsf{c}^5\,\lambda - 8\,\mu^2\,\mathsf{c}^5\right)[v_x]\,\mathrm{d}_l\theta$

$\quad + \left(\mu\,\mathsf{s}\,\lambda - 6\,\mu\,\mathsf{s}\,\mathsf{c}^2\,\lambda + 2\,\mu^2\,\mathsf{s} - 8\,\mu^2\,\mathsf{s}\,\mathsf{c}^2 + 8\,\mu\,\mathsf{c}^4\,\lambda\,\mathsf{s} + 8\,\mu^2\,\mathsf{s}\,\mathsf{c}^4\right)[v_y]\,\mathrm{d}_l\theta$

$\quad - \left(\left(8\,\mu\,\mathsf{s}\,\mathsf{c} - 16\,\mu\,\mathsf{s}\,\mathsf{c}^3 + 8\,\mu\,\mathsf{s}\,\mathsf{c}^5 - 12\,\mathsf{s}\,\mathsf{c}^3\,\lambda + 8\,\mathsf{s}\,\mathsf{c}^5\,\lambda + 4\,\mathsf{s}\,\mathsf{c}\,\lambda\right)[\mu] + \left(-2\,\mu\,\mathsf{s}\,\mathsf{c}^3 + 2\,\mu\,\mathsf{s}\,\mathsf{c}\right)[\lambda]\right)u_{xx}^-$

$\quad - \left(8\,\mu\,\mathsf{s}\,\mathsf{c}^3 - 8\,\mu\,\mathsf{s}\,\mathsf{c}^5 + 6\,\mathsf{s}\,\mathsf{c}^3\,\lambda - 8\,\mathsf{s}\,\mathsf{c}^5\,\lambda\right)[\mu]\,u_{yy}^-$

$\quad + \left(\left(11\,\mathsf{c}^2\,\lambda + 16\,\mu\,\mathsf{c}^2 - 32\,\mu\,\mathsf{c}^4 - \lambda - 2\,\mu - 26\,\mathsf{c}^4\,\lambda + 16\,\mathsf{c}^6 + 16\,\mu\,\mathsf{c}^6\right)[\mu] + \left(\mu\,\mathsf{c}^2\,[\lambda] - 2\,\mu\,\mathsf{c}^4\,[\lambda]\right)[\lambda]\right)u_{xy}^-$

$\quad + \left(12\,\mu\,\mathsf{c}^2 - 18\,\mu\,\mathsf{c}^4 + 8\,\mu\,\mathsf{c}^6 - \lambda - 2\,\mu + 8\,\mathsf{c}^6\,\lambda + 9\,\mathsf{c}^2\,\lambda - 16\,\mathsf{c}^4\,\lambda\right)[\mu]\,v_{xx}^-$

$\quad + \left(\left(10\,\mu\,\mathsf{c}^4 - 8\,\mu\,\mathsf{c}^6 - 2\,\mu\,\mathsf{c}^2 - 2\,\mathsf{c}^2\,\lambda + 10\,\mathsf{c}^4\,\lambda - 8\,\mathsf{c}^6\,\lambda\right)[\mu] + \left(+\mu\,\mathsf{c}^2 - 2\,\mu\,\mathsf{c}^4\right)[\lambda]\right)v_{yy}^-$

$\quad - \left(\left(-4\,\mu\,\mathsf{s}\,\mathsf{c} + 20\,\mu\,\mathsf{s}\,\mathsf{c}^3 - 16\,\mu\,\mathsf{s}\,\mathsf{c}^5 + 18\,\mathsf{s}\,\mathsf{c}^3\,\lambda - 4\,\mathsf{s}\,\mathsf{c}\,\lambda - 16\,\mathsf{s}\,\mathsf{c}^5\,\lambda\right)[\mu] + \left(2\,\mu\,\mathsf{s}\,\mathsf{c}\,[\lambda] - 2\,\mu\,\mathsf{s}\,\mathsf{c}^3\,[\lambda]\right)[\lambda]\right)v_{xy}^-$

$\quad - \mu\,\lambda\,\mathrm{d}_{ll}\bar{v} - 2\,\mu^2\,\mathrm{d}_{ll}\bar{v} - 4\,\mu\,\mathsf{s}\,[\mu]\,\mathrm{d}_l\theta\,u_x^- - 8\,\mu^2\,\mathrm{d}_{ll}\bar{v}\,\mathsf{c}^4 - 18\,\mu\,\mathsf{s}\,[\mu]\,\mathrm{d}_l\theta\,v_y^-\,\mathsf{c}^2$

$\quad + 4\,\mu\,\mathsf{s}\,[\mu]\,\mathrm{d}_l\theta\,v_y^- + 6\,[\mu]\,\mathrm{d}_l\theta\,\mathsf{c}\,v_x^-\,\lambda + 16\,[\mu]\,\mathrm{d}_l\theta\,\mathsf{c}^5\,v_x^-\,\lambda - 22\,[\mu]\,\mathrm{d}_l\theta\,\mathsf{c}^3\,u_y^-\,\lambda + 16\,[\mu]\,\mathrm{d}_l\theta\,\mathsf{c}^5\,u_y^-\,\lambda$

$\quad - 22\,[\mu]\,\mathrm{d}_l\theta\,\mathsf{c}^3\,v_x^-\,\lambda + 6\,[\mu]\,\mathrm{d}_l\theta\,\mathsf{c}\,u_y^-\,\lambda - 6\,\mu\,\mathsf{s}\,\mathsf{c}\,\mathrm{d}_{ll}\bar{u}\,\lambda + \mathsf{c}\,\lambda\,\mathrm{d}_l(\mathbf{g}\cdot\mathbf{n}) - \mathsf{c}^3\,\mathrm{d}_l(\mathbf{g}\cdot\mathbf{n})\,\lambda$

$\quad - \mathsf{c}^2\,\lambda\,f_2 + 8\,\mu\,[\mu]\,\mathrm{d}_l\theta\,\mathsf{c}\,u_y^- - 26\,\mu\,[\mu]\,\mathrm{d}_l\theta\,\mathsf{c}^3\,u_y^- + 8\,\mu\,[\mu]\,\mathrm{d}_l\theta\,\mathsf{c}\,v_x^- - 26\,\mu\,[\mu]\,\mathrm{d}_l\theta\,\mathsf{c}^3\,v_x^-$

$\quad - 2\,\mathsf{s}\,\lambda\,[\mu]\,\mathrm{d}_l\theta\,u_x^- + 8\,\mu\,\lambda\,\mathrm{d}_{ll}\bar{v}\,\mathsf{c}^2 + \mathsf{s}\,\mathsf{c}\,f_1\,\lambda + \mathsf{s}\,\lambda\,\mathrm{d}_l(\mathbf{g}\cdot\mathbf{t}) + 2\,\mu\,\mathsf{s}\,\mathrm{d}_l(\mathbf{g}\cdot\mathbf{t}) + \mu\,\mathsf{c}^4\,f_2$

$\quad - \mu\,\mathsf{c}^2\,f_2 + 10\,\mu^2\,\mathrm{d}_{ll}\bar{v}\,\mathsf{c}^2 + 18\,\mu\,\mathsf{s}\,[\mu]\,\mathrm{d}_l\theta\,u_x^-\,\mathsf{c}^2 - 14\,\mathsf{s}\,[\mu]\,\mathrm{d}_l\theta\,v_y^-\,\mathsf{c}^2\,\lambda$

$\quad + 14\,\mathsf{s}\,\lambda\,[\mu]\,\mathrm{d}_l\theta\,u_x^-\,\mathsf{c}^2 + 2\,\mathsf{s}\,[\mu]\,\mathrm{d}_l\theta\,v_y^-\,\lambda - 8\,\mu^2\,\mathsf{s}\,\mathsf{c}\,\mathrm{d}_{ll}\bar{u} - \mathsf{s}\,\mathsf{c}^3\,f_1\,\lambda - \mu\,\mathsf{s}\,\mathsf{c}^3\,f_1$

$\quad + 2\,\mu\,\mathsf{s}\,\mathsf{c}\,f_1 + 8\,\mu^2\,\mathsf{s}\,\mathsf{c}^3\,\mathrm{d}_{ll}\bar{u} + \mathsf{c}^4\,\lambda\,f_2 + 16\,\mathsf{s}\,\mathsf{c}^4\,\lambda\,[\mu]\,\mathrm{d}_l\theta\,v_y^- - 16\,\mathsf{s}\,\mathsf{c}^4\,\lambda\,[\mu]\,\mathrm{d}_l\theta\,u_x^-$

$\quad - 3\,\mathsf{s}\,\mathsf{c}^2\,\lambda\,\mathrm{d}_l(\mathbf{g}\cdot\mathbf{t}) - 5\,\mu\,\mathsf{s}\,\mathsf{c}^2\,\mathrm{d}_l(\mathbf{g}\cdot\mathbf{t}) + \mu\,\mathsf{c}^3\,\mathrm{d}_l(\mathbf{g}\cdot\mathbf{n}) + 8\,\mu\,\mathsf{s}\,\mathsf{c}^3\,\mathrm{d}_{ll}\bar{u}\,\lambda$

$\quad + 16\,\mu\,\mathsf{s}\,[\mu]\,\mathrm{d}_l\theta\,v_y^-\,\mathsf{c}^4 - 16\,\mu\,\mathsf{s}\,\mathsf{c}^4\,[\mu]\,\mathrm{d}_l\theta\,u_x^- + 16\,\mu\,[\mu]\,\mathrm{d}_l\theta\,\mathsf{c}^5\,v_x^- + 16\,\mu\,[\mu]\,\mathrm{d}_l\theta\,\mathsf{c}^5\,u_y^- - 8\,\mu\,\mathsf{c}^4\,\lambda\,\mathrm{d}_{ll}\bar{v}$

$\mu(2\mu + \lambda)[u_{yy}] =$

$\left(7\,\mu\,\lambda\,\mathsf{c} - 14\,\mu\,\mathsf{c}^3\,\lambda - 16\,\mathsf{c}^3\,\mu^2 + 10\,\mu^2\,\mathsf{c} + 8\,\mu^2\,\mathsf{c}^5 + 8\,\mu\,\mathsf{c}^5\,\lambda\right)[u_x]\,\mathrm{d}_l\theta$

$- \left(\mu\,\mathsf{s}\,\lambda - 8\,\mu^2\,\mathsf{s}\,\mathsf{c}^4 + 8\,\mu^2\,\mathsf{s}\,\mathsf{c}^2 + 6\,\mu\,\mathsf{s}\,\mathsf{c}^2\,\lambda + 2\,\mu^2\,\mathsf{s} - 8\,\mu\,\mathsf{c}^4\,\lambda\,\mathsf{s}\right)[u_y]\,\mathrm{d}_l\theta$

$+ \left(8\,\mu^2\,\mathsf{s}\,\mathsf{c}^4 + 2\,\mu\,\mathsf{s}\,\lambda - 12\,\mu\,\mathsf{s}\,\mathsf{c}^2\,\lambda - 14\,\mu^2\,\mathsf{s}\,\mathsf{c}^2 + 2\,\mu^2\,\mathsf{s} + 8\,\mu\,\mathsf{c}^4\,\lambda\,\mathsf{s}\right)[v_x]\,\mathrm{d}_l\theta$

$- \left(6\,\mu^2\,\mathsf{c} - 14\,\mathsf{c}^3\,\mu^2 + 8\,\mu^2\,\mathsf{c}^5 - 12\,\mu\,\mathsf{c}^3\,\lambda + 8\,\mu\,\mathsf{c}^5\,\lambda + 4\,\mu\,\lambda\,\mathsf{c}\right)[v_y]\,\mathrm{d}_l\theta$

$- \left(\left(22\,\mu\,\mathsf{c}^4 - 8\,\mu\,\mathsf{c}^6 + 4\,\mu + 18\,\mathsf{c}^4\,\lambda - 8\,\mathsf{c}^6\,\lambda - 12\,\mathsf{c}^2\,\lambda + 2\,\lambda - 18\,\mu\,\mathsf{c}^2\right)[\mu] + \left(\mu + 2\,\mu\,\mathsf{c}^4 - 3\,\mu\,\mathsf{c}^2\right)[\lambda]\right)u_{xx}^-$

$+ \left(14\,\mu\,\mathsf{c}^4 - 8\,\mu\,\mathsf{c}^6 - 2\,\mu\,[\mu] - 8\,\mathsf{c}^6\,\lambda + 12\,\mathsf{c}^4\,\lambda - 3\,\mathsf{c}^2\,\lambda - \lambda - 4\,\mu\,\mathsf{c}^2\right)[\mu]\,u_{yy}^-$

$+ \left(\left(8\,\mu\,\mathsf{s}\,\mathsf{c} - 28\,\mu\,\mathsf{s}\,\mathsf{c}^3 + 6\,\mathsf{s}\,\mathsf{c}\,\lambda - 22\,\mathsf{s}\,\mathsf{c}^3\,\lambda + 16\,\mathsf{s}\,\mathsf{c}^5\,\lambda + 16\,\mu\,\mathsf{s}\,\mathsf{c}^5\right)[\mu] - 2\,\mu\,\mathsf{s}\,\mathsf{c}^3\,[\lambda]\right)u_{xy}^-$

$+ \left(8\,\mu\,\mathsf{s}\,\mathsf{c} - 16\,\mu\,\mathsf{s}\,\mathsf{c}^3 + 8\,\mu\,\mathsf{s}\,\mathsf{c}^5 + 6\,\mathsf{s}\,\mathsf{c}\,\lambda - 14\,\mathsf{s}\,\mathsf{c}^3\,\lambda + 8\,\mathsf{s}\,\mathsf{c}^5\,\lambda\right)[\mu]\,v_{xx}^-$

$+ \left(\left(8\,\mu\,\mathsf{s}\,\mathsf{c}^3 - 8\,\mu\,\mathsf{s}\,\mathsf{c}^5 + 8\,\mathsf{s}\,\mathsf{c}^3\,\lambda - 8\,\mathsf{s}\,\mathsf{c}^5\,\lambda\right)[\mu] - 2\,\mu\,\mathsf{s}\,\mathsf{c}^3\,[\lambda]\right)v_{yy}^-$

$+ \left(\left(32\,\mu\,\mathsf{c}^4 - 16\,\mu\,\mathsf{c}^6 - 16\,\mathsf{c}^6\,\lambda - 15\,\mathsf{c}^2\,\lambda + 30\,\mathsf{c}^4\,\lambda + \lambda - 16\,\mu\,\mathsf{c}^2\right)[\mu] + \left(-\mu\,[\lambda] - 2\,\mu\,\mathsf{c}^4 + 3\,\mu\,\mathsf{c}^2\right)[\lambda]\right)v_{xy}^-$

$+ 2\,\mu\,f_1 + 2\,\mu\,\mathsf{s}\,\mathrm{d}_l\theta\,[\mu]\,u_y^- + 2\,\mathsf{s}\,\lambda\,\mathrm{d}_l\theta\,[\mu]\,u_y^- + \mu\,\mathsf{s}\,\mathrm{d}_l(\mathbf{g}\cdot\mathbf{n}) + \mathsf{s}\,\lambda\,\mathrm{d}_l(\mathbf{g}\cdot\mathbf{n}) - \mathsf{s}\,\mathsf{c}\,\lambda\,f_2$

$- \mu\,\mathsf{s}\,\mathsf{c}\,f_2 + 2\,\mu\,\mathsf{s}\,\mathrm{d}_l\theta\,[\mu]\,v_x^- + 2\,\mathsf{s}\,\lambda\,th\,[\mu]\,v_x^- + 3\,\mathsf{c}^3\,\mathrm{d}_l(\mathbf{g}\cdot\mathbf{t})\,\lambda + f_1\,\lambda - 16\,[\mu]\,\mathrm{d}_l\theta\,v_y^-\,\mathsf{c}^5\,\lambda$

$+ 16\,\mu\,\mathsf{s}\,[\mu]\,\mathrm{d}_l\theta\,\mathsf{c}^4\,u_y^- + 16\,\mu\,[\mu]\,\mathrm{d}_l\theta\,u_x^-\,\mathsf{c}^5 - 16\,\mu\,[\mu]\,\mathrm{d}_l\theta\,v_y^-\,\mathsf{c}^5 + 16\,\mu\,\mathsf{s}\,[\mu]\,\mathrm{d}_l\theta\,\mathsf{c}^4\,v_x^- - 8\,\mu\,\mathsf{s}\,\mathsf{c}^3\,\mathrm{d}_{ll}\bar{v}\,\lambda$

$+ 5\,\mu\,\mathsf{c}^3\,\mathrm{d}_l(\mathbf{g}\cdot\mathbf{t}) - 3\,\mu\,\lambda\,\mathrm{d}_{ll}\bar{u} - 8\,\mu^2\,\mathsf{s}\,\mathsf{c}^3\,\mathrm{d}_{ll}\bar{v} + 16\,[\mu]\,\mathrm{d}_l\theta\,u_x^-\,\mathsf{c}^5\,\lambda + 16\,\mathsf{s}\,[\mu]\,\mathrm{d}_l\theta\,\mathsf{c}^4\,u_y^-\,\lambda$

$+ 16\,\mathsf{s}\,[\mu]\,\mathrm{d}_l\theta\,\mathsf{c}^4\,v_x^-\,\lambda - 8\,\mu\,\mathsf{c}^4\,\lambda\,\mathrm{d}_{ll}\bar{u} + \mu\,\mathsf{s}\,\mathsf{c}^2\,\mathrm{d}_l(\mathbf{g}\cdot\mathbf{n}) - \mathsf{s}\,\mathsf{c}^2\,\mathrm{d}_l(\mathbf{g}\cdot\mathbf{n})\,\lambda - 4\,\mu^2\,\mathrm{d}_{ll}\bar{u}$

$+ 12\,\mu\,\mathsf{c}^2\,\lambda\,\mathrm{d}_{ll}\bar{u} + \mu\,\mathsf{s}\,\mathsf{c}^3\,f_2 + 8\,\mu^2\,\mathsf{s}\,\mathsf{c}\,\mathrm{d}_{ll}\bar{v} + \mathsf{s}\,\mathsf{c}^3\,\lambda\,f_2 + 10\,\mathsf{c}\,[\mu]\,\mathrm{d}_l\theta\,u_x^-\,\lambda - 10\,\mathsf{c}\,[\mu]\,\mathrm{d}_l\theta\,v_y^-\,\lambda$

$+ 26\,[\mu]\,\mathrm{d}_l\theta\,v_y^-\,\mathsf{c}^3\,\lambda - 26\,[\mu]\,\mathrm{d}_l\theta\,u_x^-\,\mathsf{c}^3\,\lambda - 30\,\mu\,[\mu]\,\mathrm{d}_l\theta\,u_x^-\,\mathsf{c}^3 + 30\,\mu\,[\mu]\,\mathrm{d}_l\theta\,v_y^-\,\mathsf{c}^3 - 14\,\mu\,\mathsf{c}\,[\mu]\,\mathrm{d}_l\theta\,v_y^-$

$+ 14\,\mu\,\mathsf{c}\,[\mu]\,\mathrm{d}_l\theta\,u_x^- - 18\,\mathsf{s}\,[\mu]\,\mathrm{d}_l\theta\,\mathsf{c}^2\,u_y^-\,\lambda - 18\,\mathsf{s}\,[\mu]\,\mathrm{d}_l\theta\,\mathsf{c}^2\,v_x^-\,\lambda + 6\,\mu\,\mathsf{s}\,\mathsf{c}\,\mathrm{d}_{ll}\bar{v}\,\lambda$

$- 22\,\mu\,\mathsf{s}\,[\mu]\,\mathrm{d}_l\theta\,\mathsf{c}^2\,u_y^- - 22\,\mu\,\mathsf{s}\,[\mu]\,\mathrm{d}_l\theta\,\mathsf{c}^2\,v_x^- - 3\,\mu\,\mathsf{c}^2\,f_1 - 2\,\mathsf{c}^2\,f_1\,\lambda + \mathsf{c}^4\,f_1\,\lambda - 3\,\mathsf{c}\,\lambda\,\mathrm{d}_l(\mathbf{g}\cdot\mathbf{t})$

$- 5\,\mu\,\mathsf{c}\,\mathrm{d}_l(\mathbf{g}\cdot\mathbf{t}) + \mu\,\mathsf{c}^4\,f_1 + 14\,\mu^2\,\mathrm{d}_{ll}\bar{u}\,\mathsf{c}^2 - 8\,\mathsf{c}^4\,\mu^2\,\mathrm{d}_{ll}\bar{u}$

References

[1] J. Aboudi. *Mechanics of Composite Materials*. Elsevier, 1991.

[2] G. Allaire. *Shape Optimization by the Homogenization Method*. Springer, 2002.

[3] R. J. LeVeque and Z. Li. The Immersed Interface Method for Elliptic Equations with Discontinuous Coefficients and Singular Sources. *SIAM J. Numer. Anal.*, 31:1019—1044, 1994.

[4] Z. Li. A Fast Iterative Algorithm for Elliptic Interface Problems. *SIAM J. Numer. Anal.*, 35(1):230—254, 1998.

[5] A. Mayo. The fast solution of Poisson's and the biharmonic equations on irregular regions. *SIAM J. Numer. Anal.*, 21(2):285—299, 1984.

[6] S. J. Osher and J. A. Sethian. Fronts propagating with curvature dependent speed: Algorithms based on the Hamilton-Jacobi formulation. *Journal of Computational Physics*, 79:12—49, 1988.

[7] V. Rutka. A Fast Numerical Method for the Computation of Effective Elastic Moduli of 3D Fibrous Microstructures. Master's thesis, University of Kaiserslautern, August 2001.

[8] V. Rutka. *Immersed Interface Methods for Elliptic Boundary Value Problems*. PhD thesis, Technische Universität Kaiserslautern, 2005. submitted.

[9] V. Rutka, A. Wiegmann, and H. Andrä. EJIIM for Calculation of Effective Elastic Moduli in 3D Linear Elasticity. In preparation.

[10] J. A. Sethian and A. Wiegmann. Structural Boundary Design via Level Set and Explicit Jump Immersed Interface Methods. *J. Comp. Phys.*, 163(2):489—528, 2000.

[11] A. Wiegmann. Fast Poisson, fast Helmholtz and fast linear elastostatic solvers on rectangular parallelepipeds. Technical Report LBNL-43565, Lawrence Berkeley National Laboratory, MS 50A-1148, One Cyclotron Rd, Berkeley CA 94720, June 1999. Submitted.

[12] A. Wiegmann and K. P. Bube. The Explicit-Jump Immersed Interface Method: Finite Difference Methods for PDEs with Piecewise Smooth Solutions. *SIAM J. Numer. Anal.*, 37(3):827—862, 2000.

[13] X. Yang, B. Li, and Z. Li. The Immersed Interface Method for Elasticity Problems with Interface. *Discrete and Impulsive Systems, Part B*, 10(5):783—808, 2003.

Published reports of the Fraunhofer ITWM

The PDF-files of the following reports are available under:
www.itwm.fraunhofer.de/de/zentral__berichte/berichte

1. D. Hietel, K. Steiner, J. Struckmeier

A Finite - Volume Particle Method for Compressible Flows

We derive a new class of particle methods for conservation laws, which are based on numerical flux functions to model the interactions between moving particles. The derivation is similar to that of classical Finite-Volume methods; except that the fixed grid structure in the Finite-Volume method is substituted by so-called mass packets of particles. We give some numerical results on a shock wave solution for Burgers equation as well as the well-known one-dimensional shock tube problem.
(19 pages, 1998)

2. M. Feldmann, S. Seibold

Damage Diagnosis of Rotors: Application of Hilbert Transform and Multi-Hypothesis Testing

In this paper, a combined approach to damage diagnosis of rotors is proposed. The intention is to employ signal-based as well as model-based procedures for an improved detection of size and location of the damage. In a first step, Hilbert transform signal processing techniques allow for a computation of the signal envelope and the instantaneous frequency, so that various types of non-linearities due to a damage may be identified and classified based on measured response data. In a second step, a multi-hypothesis bank of Kalman Filters is employed for the detection of the size and location of the damage based on the information of the type of damage provided by the results of the Hilbert transform.
Keywords: Hilbert transform, damage diagnosis, Kalman filtering, non-linear dynamics
(23 pages, 1998)

3. Y. Ben-Haim, S. Seibold

Robust Reliability of Diagnostic Multi-Hypothesis Algorithms: Application to Rotating Machinery

Damage diagnosis based on a bank of Kalman filters, each one conditioned on a specific hypothesized system condition, is a well recognized and powerful diagnostic tool. This multi-hypothesis approach can be applied to a wide range of damage conditions. In this paper, we will focus on the diagnosis of cracks in rotating machinery. The question we address is: how to optimize the multi-hypothesis algorithm with respect to the uncertainty of the spatial form and location of cracks and their resulting dynamic effects. First, we formulate a measure of the reliability of the diagnostic algorithm, and then we discuss modifications of the diagnostic algorithm for the maximization of the reliability. The reliability of a diagnostic algorithm is measured by the amount of uncertainty consistent with no-failure of the diagnosis. Uncertainty is quantitatively represented with convex models.
Keywords: Robust reliability, convex models, Kalman filtering, multi-hypothesis diagnosis, rotating machinery, crack diagnosis
(24 pages, 1998)

4. F.-Th. Lentes, N. Siedow

Three-dimensional Radiative Heat Transfer in Glass Cooling Processes

For the numerical simulation of 3D radiative heat transfer in glasses and glass melts, practically applicable mathematical methods are needed to handle such problems optimal using workstation class computers. Since the exact solution would require super-computer capabilities we concentrate on approximate solutions with a high degree of accuracy. The following approaches are studied: 3D diffusion approximations and 3D ray-tracing methods.
(23 pages, 1998)

5. A. Klar, R. Wegener

A hierarchy of models for multilane vehicular traffic
Part I: Modeling

In the present paper multilane models for vehicular traffic are considered. A microscopic multilane model based on reaction thresholds is developed. Based on this model an Enskog like kinetic model is developed. In particular, care is taken to incorporate the correlations between the vehicles. From the kinetic model a fluid dynamic model is derived. The macroscopic coefficients are deduced from the underlying kinetic model. Numerical simulations are presented for all three levels of description in [10]. Moreover, a comparison of the results is given there.
(23 pages, 1998)

Part II: Numerical and stochastic investigations

In this paper the work presented in [6] is continued. The present paper contains detailed numerical investigations of the models developed there. A numerical method to treat the kinetic equations obtained in [6] are presented and results of the simulations are shown. Moreover, the stochastic correlation model used in [6] is described and investigated in more detail.
(17 pages, 1998)

6. A. Klar, N. Siedow

Boundary Layers and Domain Decomposition for Radiative Heat Transfer and Diffusion Equations: Applications to Glass Manufacturing Processes

In this paper domain decomposition methods for radiative transfer problems including conductive heat transfer are treated. The paper focuses on semi-transparent materials, like glass, and the associated conditions at the interface between the materials. Using asymptotic analysis we derive conditions for the coupling of the radiative transfer equations and a diffusion approximation. Several test cases are treated and a problem appearing in glass manufacturing processes is computed. The results clearly show the advantages of a domain decomposition approach. Accuracy equivalent to the solution of the global radiative transfer solution is achieved, whereas computation time is strongly reduced.
(24 pages, 1998)

7. I. Choquet

Heterogeneous catalysis modelling and numerical simulation in rarified gas flows Part I: Coverage locally at equilibrium

A new approach is proposed to model and simulate numerically heterogeneous catalysis in rarefied gas flows. It is developed to satisfy all together the following points:
1) describe the gas phase at the microscopic scale, as required in rarefied flows,
2) describe the wall at the macroscopic scale, to avoid prohibitive computational costs and consider not only crystalline but also amorphous surfaces,
3) reproduce on average macroscopic laws correlated with experimental results and
4) derive analytic models in a systematic and exact way. The problem is stated in the general framework of a non static flow in the vicinity of a catalytic and non porous surface (without aging). It is shown that the exact and systematic resolution method based on the Laplace transform, introduced previously by the author to model collisions in the gas phase, can be extended to the present problem. The proposed approach is applied to the modelling of the EleyRideal and LangmuirHinshelwood recombinations, assuming that the coverage is locally at equilibrium. The models are developed considering one atomic species and extended to the general case of several atomic species. Numerical calculations show that the models derived in this way reproduce with accuracy behaviors observed experimentally.
(24 pages, 1998)

8. J. Ohser, B. Steinbach, C. Lang

Efficient Texture Analysis of Binary Images

A new method of determining some characteristics of binary images is proposed based on a special linear filtering. This technique enables the estimation of the area fraction, the specific line length, and the specific integral of curvature. Furthermore, the specific length of the total projection is obtained, which gives detailed information about the texture of the image. The influence of lateral and directional resolution depending on the size of the applied filter mask is discussed in detail. The technique includes a method of increasing directional resolution for texture analysis while keeping lateral resolution as high as possible.
(17 pages, 1998)

9. J. Orlik

Homogenization for viscoelasticity of the integral type with aging and shrinkage

A multiphase composite with periodic distributed inclusions with a smooth boundary is considered in this contribution. The composite component materials are supposed to be linear viscoelastic and aging (of the non-convolution integral type, for which the Laplace transform with respect to time is not effectively applicable) and are subjected to isotropic shrinkage. The free shrinkage deformation can be considered as a fictitious temperature deformation in the behavior law. The procedure presented in this paper proposes a way to determine average (effective homogenized) viscoelastic and shrinkage (temperature) composite properties and the homogenized stressfield from known properties of the components. This is done by the extension of the asymptotic homogenization technique known for pure elastic nonhomogeneous bodies to the nonhomogeneous thermoviscoelasticity of the integral nonconvolution type. Up to now, the homogenization theory has not covered viscoelasticity of the integral type. SanchezPalencia (1980), Francfort & Suquet (1987) (see [2], [9]) have considered homogenization for viscoelasticity of the differential form and only up to the first derivative order. The integralmodeled viscoelasticity is more general then the differential one and includes almost all known differential models. The homogenization procedure is based on the construction of an asymptotic solution with respect to a period of the composite structure. This reduces the original problem to some auxiliary boundary value problems of elasticity and viscoelasticity on the unit periodic cell, of the same type as the original non-homogeneous problem. The existence and uniqueness results for such problems were obtained for kernels satisfying some constrain conditions. This is done by the extension of the Volterra integral operator theory to the Volterra operators with respect to the time, whose 1 kernels are space linear operators for any fixed time variables. Some ideas of such approach were proposed in [11] and [12], where the Volterra operators with kernels depending additionally on parameter were considered. This manuscript delivers results of the same nature for the case of the spaceoperator kernels.
(20 pages, 1998)

10. J. Mohring

Helmholtz Resonators with Large Aperture

The lowest resonant frequency of a cavity resonator is usually approximated by the classical Helmholtz formula. However, if the opening is rather large and the front wall is narrow this formula is no longer valid. Here we present a correction which is of third order in the ratio of the diameters of aperture and cavity. In addition to the high accuracy it allows to estimate the damping due to radiation. The result is found by applying the method of matched asymptotic expansions. The correction contains form factors describing the shapes of opening and cavity. They are computed for a number of standard geometries. Results are compared with numerical computations.
(21 pages, 1998)

11. H. W. Hamacher, A. Schöbel

On Center Cycles in Grid Graphs

Finding "good" cycles in graphs is a problem of great interest in graph theory as well as in locational analysis. We show that the center and median problems are NP hard in general graphs. This result holds both for the variable cardinality case (i.e. all cycles of the graph are considered) and the fixed cardinality case (i.e. only cycles with a given cardinality p are feasible). Hence it is of interest to investigate special cases where the problem is solvable in polynomial time. In grid graphs, the variable cardinality case is, for instance, trivially solvable if the shape of the cycle can be chosen freely. If the shape is fixed to be a rectangle one can analyze rectangles in grid graphs with, in sequence, fixed dimension, fixed cardinality, and variable cardinality. In all cases a complete characterization of the optimal cycles and closed form expressions of the optimal objective values are given, yielding polynomial time algorithms for all cases of center rectangle problems. Finally, it is shown that center cycles can be chosen as rectangles for small cardinalities such that the center cycle problem in grid graphs is in these cases completely solved.
(15 pages, 1998)

12. H. W. Hamacher, K.-H. Küfer

Inverse radiation therapy planning - a multiple objective optimisation approach

For some decades radiation therapy has been proved successful in cancer treatment. It is the major task of clinical radiation treatment planning to realize on the one hand a high level dose of radiation in the cancer tissue in order to obtain maximum tumor control. On the other hand it is obvious that it is absolutely necessary to keep in the tissue outside the tumor, particularly in organs at risk, the unavoidable radiation as low as possible.

No doubt, these two objectives of treatment planning - high level dose in the tumor, low radiation outside the tumor - have a basically contradictory nature. Therefore, it is no surprise that inverse mathematical models with dose distribution bounds tend to be infeasible in most cases. Thus, there is need for approximations compromising between overdosing the organs at risk and underdosing the target volume.

Differing from the currently used time consuming iterative approach, which measures deviation from an ideal (non-achievable) treatment plan using recursively trial-and-error weights for the organs of interest, we go a new way trying to avoid a priori weight choices and consider the treatment planning problem as a multiple objective linear programming problem: with each organ of interest, target tissue as well as organs at risk, we associate an objective function measuring the maximal deviation from the prescribed doses.

We build up a data base of relatively few efficient solutions representing and approximating the variety of Pareto solutions of the multiple objective linear programming problem. This data base can be easily scanned by physicians looking for an adequate treatment plan with the aid of an appropriate online tool.
(14 pages, 1999)

13. C. Lang, J. Ohser, R. Hilfer

On the Analysis of Spatial Binary Images

This paper deals with the characterization of microscopically heterogeneous, but macroscopically homogeneous spatial structures. A new method is presented which is strictly based on integral-geometric formulae such as Crofton's intersection formulae and Hadwiger's recursive definition of the Euler number. The corresponding algorithms have clear advantages over other techniques. As an example of application we consider the analysis of spatial digital images produced by means of Computer Assisted Tomography.
(20 pages, 1999)

14. M. Junk

On the Construction of Discrete Equilibrium Distributions for Kinetic Schemes

A general approach to the construction of discrete equilibrium distributions is presented. Such distribution functions can be used to set up Kinetic Schemes as well as Lattice Boltzmann methods. The general prin-ciples are also applied to the construction of Chapman Enskog distributions which are used in Kinetic Schemes for compressible Navier-Stokes equations.
(24 pages, 1999)

15. M. Junk, S. V. Raghurame Rao

A new discrete velocity method for Navier-Stokes equations

The relation between the Lattice Boltzmann Method, which has recently become popular, and the Kinetic Schemes, which are routinely used in Computational Fluid Dynamics, is explored. A new discrete velocity model for the numerical solution of Navier-Stokes equations for incompressible fluid flow is presented by combining both the approaches. The new scheme can be interpreted as a pseudo-compressibility method and, for a particular choice of parameters, this interpretation carries over to the Lattice Boltzmann Method.
(20 pages, 1999)

16. H. Neunzert

Mathematics as a Key to Key Technologies

The main part of this paper will consist of examples, how mathematics really helps to solve industrial problems; these examples are taken from our Institute for Industrial Mathematics, from research in the Techno-mathematics group at my university, but also from ECMI groups and a company called TecMath, which originated 10 years ago from my university group and has already a very successful history.
(39 pages (4 PDF-Files), 1999)

17. J. Ohser, K. Sandau

Considerations about the Estimation of the Size Distribution in Wicksell's Corpuscle Problem

Wicksell's corpuscle problem deals with the estimation of the size distribution of a population of particles, all having the same shape, using a lower dimensional sampling probe. This problem was originary formulated for particle systems occurring in life sciences but its solution is of actual and increasing interest in materials science. From a mathematical point of view, Wicksell's problem is an inverse problem where the interesting size distribution is the unknown part of a Volterra equation. The problem is often regarded ill-posed, because the structure of the integrand implies unstable numerical solutions. The accuracy of the numerical solutions is considered here using the condition number, which allows to compare different numerical methods with different (equidistant) class sizes and which indicates, as one result, that a finite section thickness of the probe reduces the numerical problems. Furthermore, the relative error of estimation is computed which can be split into two parts. One part consists of the relative discretization error that increases for increasing class size, and the second part is related to the relative statistical error which increases with decreasing class size. For both parts, upper bounds can be given and the sum of them indicates an optimal class width depending on some specific constants.
(18 pages, 1999)

18. E. Carrizosa, H. W. Hamacher, R. Klein, S. Nickel

Solving nonconvex planar location problems by finite dominating sets

It is well-known that some of the classical location problems with polyhedral gauges can be solved in polynomial time by finding a finite dominating set, i. e. a finite set of candidates guaranteed to contain at least one optimal location.

In this paper it is first established that this result holds for a much larger class of problems than currently considered in the literature. The model for which this result can be proven includes, for instance, location problems with attraction and repulsion, and location-allocation problems.

Next, it is shown that the approximation of general gauges by polyhedral ones in the objective function of our general model can be analyzed with regard to the subsequent error in the optimal objective value. For the approximation problem two different approaches are described, the sandwich procedure and the greedy algorithm. Both of these approaches lead - for fixed epsilon - to polynomial approximation algorithms with accuracy epsilon for solving the general model considered in this paper.
Keywords: Continuous Location, Polyhedral Gauges, Finite Dominating Sets, Approximation, Sandwich Algorithm, Greedy Algorithm
(19 pages, 2000)

19. A. Becker

A Review on Image Distortion Measures

Within this paper we review image distortion measures. A distortion measure is a criterion that assigns a "quality number" to an image. We distinguish between mathematical distortion measures and those distortion measures in-cooperating a priori knowledge about the imaging devices (e. g. satellite images), image processing algorithms or the human physiology. We will consider representative examples of different kinds of distortion measures and are going to discuss them.
Keywords: Distortion measure, human visual system
(26 pages, 2000)

20. H. W. Hamacher, M. Labbé, S. Nickel, T. Sonneborn

Polyhedral Properties of the Uncapacitated Multiple Allocation Hub Location Problem

We examine the feasibility polyhedron of the uncapacitated hub location problem (UHL) with multiple allocation, which has applications in the fields of air passenger and cargo transportation, telecommunication and postal delivery services. In particular we determine the dimension and derive some classes of facets of this polyhedron. We develop some general rules about lifting facets from the uncapacitated facility location (UFL) for UHL and projecting facets from UHL to UFL. By applying these rules we get a new class of facets for UHL which dominates the inequalities in the original formulation. Thus we get a new formulation of UHL whose constraints are all facet–defining. We show its superior computational performance by benchmarking it on a well known data set.
Keywords: integer programming, hub location, facility location, valid inequalities, facets, branch and cut
(21 pages, 2000)

21. H. W. Hamacher, A. Schöbel

Design of Zone Tariff Systems in Public Transportation

Given a public transportation system represented by its stops and direct connections between stops, we consider two problems dealing with the prices for the customers: The fare problem in which subsets of stops are already aggregated to zones and "good" tariffs have to be found in the existing zone system. Closed form solutions for the fare problem are presented for three objective functions. In the zone problem the design of the zones is part of the problem. This problem is NP hard and we therefore propose three heuristics which prove to be very successful in the redesign of one of Germany's transportation systems.
(30 pages, 2001)

22. D. Hietel, M. Junk, R. Keck, D. Teleaga

The Finite-Volume-Particle Method for Conservation Laws

In the Finite-Volume-Particle Method (FVPM), the weak formulation of a hyperbolic conservation law is discretized by restricting it to a discrete set of test functions. In contrast to the usual Finite-Volume approach, the test functions are not taken as characteristic functions of the control volumes in a spatial grid, but are chosen from a partition of unity with smooth and overlapping partition functions (the particles), which can even move along pre- scribed velocity fields. The information exchange between particles is based on standard numerical flux functions. Geometrical information, similar to the surface area of the cell faces in the Finite-Volume Method and the corresponding normal directions are given as integral quantities of the partition functions. After a brief derivation of the Finite-Volume-Particle Method, this work focuses on the role of the geometric coefficients in the scheme.
(16 pages, 2001)

23. T. Bender, H. Hennes, J. Kalcsics, M. T. Melo, S. Nickel

Location Software and Interface with GIS and Supply Chain Management

The objective of this paper is to bridge the gap between location theory and practice. To meet this objective focus is given to the development of software capable of addressing the different needs of a wide group of users. There is a very active community on location theory encompassing many research fields such as operations research, computer science, mathematics, engineering, geography, economics and marketing. As a result, people working on facility location problems have a very diverse background and also different needs regarding the software to solve these problems. For those interested in non-commercial applications (e. g. students and researchers), the library of location algorithms (LoLA can be of considerable assistance. LoLA contains a collection of efficient algorithms for solving planar, network and discrete facility location problems. In this paper, a detailed description of the functionality of LoLA is presented. In the fields of geography and marketing, for instance, solving facility location problems requires using large amounts of demographic data. Hence, members of these groups (e. g. urban planners and sales managers) often work with geographical information too s. To address the specific needs of these users, LoLA was inked to a geographical information system (GIS) and the details of the combined functionality are described in the paper. Finally, there is a wide group of practitioners who need to solve large problems and require special purpose software with a good data interface. Many of such users can be found, for example, in the area of supply chain management (SCM). Logistics activities involved in strategic SCM include, among others, facility location planning. In this paper, the development of a commercial location software tool is also described. The too is embedded in the Advanced Planner and Optimizer SCM software developed by SAP AG, Walldorf, Germany. The paper ends with some conclusions and an outlook to future activities.
Keywords: facility location, software development, geographical information systems, supply chain management
(48 pages, 2001)

24. H. W. Hamacher, S. A. Tjandra

Mathematical Modelling of Evacuation Problems: A State of Art

This paper details models and algorithms which can be applied to evacuation problems. While it concentrates on building evacuation many of the results are applicable also to regional evacuation. All models consider the time as main parameter, where the travel time between components of the building is part of the input and the overall evacuation time is the output. The paper distinguishes between macroscopic and microscopic evacuation models both of which are able to capture the evacuees' movement over time. Macroscopic models are mainly used to produce good lower bounds for the evacuation time and do not consider any individual behavior during the emergency situation. These bounds can be used to analyze existing buildings or help in the design phase of planning a building. Macroscopic approaches which are based on dynamic network flow models (minimum cost dynamic flow, maximum dynamic flow, universal maximum flow, quickest path and quickest flow) are described. A special feature of the presented approach is the fact, that travel times of evacuees are not restricted to be constant, but may be density dependent. Using multicriteria optimization priority regions and blockage due to fire or smoke may be considered. It is shown how the modelling can be done using time parameter either as discrete or continuous parameter.
Microscopic models are able to model the individual evacuee's characteristics and the interaction among evacuees which influence their movement. Due to the corresponding huge amount of data one uses simulation approaches. Some probabilistic laws for individual evacuee's movement are presented. Moreover ideas to model the evacuee's movement using cellular automata (CA) and resulting software are presented. In this paper we will focus on macroscopic models and only summarize some of the results of the microscopic

approach. While most of the results are applicable to general evacuation situations, we concentrate on building evacuation.
(44 pages, 2001)

25. J. Kuhnert, S. Tiwari

Grid free method for solving the Poisson equation

A Grid free method for solving the Poisson equation is presented. This is an iterative method. The method is based on the weighted least squares approximation in which the Poisson equation is enforced to be satisfied in every iterations. The boundary conditions can also be enforced in the iteration process. This is a local approximation procedure. The Dirichlet, Neumann and mixed boundary value problems on a unit square are presented and the analytical solutions are compared with the exact solutions. Both solutions matched perfectly.
Keywords: Poisson equation, Least squares method, Grid free method
(19 pages, 2001)

26. T. Götz, H. Rave, D. Reinel-Bitzer, K. Steiner, H. Tiemeier

Simulation of the fiber spinning process

To simulate the influence of process parameters to the melt spinning process a fiber model is used and coupled with CFD calculations of the quench air flow. In the fiber model energy, momentum and mass balance are solved for the polymer mass flow. To calculate the quench air the Lattice Boltzmann method is used. Simulations and experiments for different process parameters and hole configurations are compared and show a good agreement.
Keywords: Melt spinning, fiber model, Lattice Boltzmann, CFD
(19 pages, 2001)

27. A. Zemitis

On interaction of a liquid film with an obstacle

In this paper mathematical models for liquid films generated by impinging jets are discussed. Attention is stressed to the interaction of the liquid film with some obstacle. S. G. Taylor [Proc. R. Soc. London Ser. A 253, 313 (1959)] found that the liquid film generated by impinging jets is very sensitive to properties of the wire which was used as an obstacle. The aim of this presentation is to propose a modification of the Taylor's model, which allows to simulate the film shape in cases, when the angle between jets is different from 180°. Numerical results obtained by discussed models give two different shapes of the liquid film similar as in Taylors experiments. These two shapes depend on the regime: either droplets are produced close to the obstacle or not. The difference between two regimes becomes larger if the angle between jets decreases. Existence of such two regimes can be very essential for some applications of impinging jets, if the generated liquid film can have a contact with obstacles.
Keywords: impinging jets, liquid film, models, numerical solution, shape
(22 pages, 2001)

28. I. Ginzburg, K. Steiner

Free surface lattice-Boltzmann method to model the filling of expanding cavities by Bingham Fluids

The filling process of viscoplastic metal alloys and plastics in expanding cavities is modelled using the lattice Boltzmann method in two and three dimensions. These models combine the regularized Bingham model for viscoplastic with a free-interface algorithm. The latter is based on a modified immiscible lattice Boltzmann model in which one species is the fluid and the other one is considered as vacuum. The boundary conditions at the curved liquid-vacuum interface are met without any geometrical front reconstruction from a first-order Chapman-Enskog expansion. The numerical results obtained with these models are found in good agreement with available theoretical and numerical analysis. Keywords: Generalized LBE, free-surface phenomena,

interface boundary conditions, filling processes, Bingham viscoplastic model, regularized models
(22 pages, 2001)

29. H. Neunzert

»Denn nichts ist für den Menschen als Menschen etwas wert, was er nicht mit Leidenschaft tun kann«
Vortrag anlässlich der Verleihung des Akademiepreises des Landes Rheinland-Pfalz am 21.11.2001

Was macht einen guten Hochschullehrer aus? Auf diese Frage gibt es sicher viele verschiedene, fachbezogene Antworten, aber auch ein paar allgemeine Gesichtspunkte: es bedarf der »Leidenschaft« für die Forschung (Max Weber), aus der dann auch die Begeisterung für die Lehre erwächst. Forschung und Lehre gehören zusammen, um die Wissenschaft als lebendiges Tun vermitteln zu können. Der Vortrag gibt Beispiele dafür, wie in angewandter Mathematik Forschungsaufgaben aus praktischen Alltagsproblemstellungen erwachsen, die in die Lehre auf verschiedenen Stufen (Gymnasium bis Graduiertenkolleg) einfließen; er leitet damit auch zu einem aktuellen Forschungsgebiet, der Mehrskalenanalyse mit ihren vielfältigen Anwendungen in Bildverarbeitung, Materialentwicklung und Strömungsmechanik über, was aber nur kurz gestreift wird. Mathematik erscheint hier als eine moderne Schlüsseltechnologie, die aber auch enge Beziehungen zu den Geistes- und Sozialwissenschaften hat.
Keywords: Lehre, Forschung, angewandte Mathematik, Mehrskalenanalyse, Strömungsmechanik
(18 pages, 2001)

30. J. Kuhnert, S. Tiwari

Finite pointset method based on the projection method for simulations of the incompressible Navier-Stokes equations

A Lagrangian particle scheme is applied to the projection method for the incompressible Navier-Stokes equations. The approximation of spatial derivatives is obtained by the weighted least squares method. The pressure Poisson equation is solved by a local iterative procedure with the help of the least squares method. Numerical tests are performed for two dimensional cases. The Couette flow, Poiseuelle flow, decaying shear flow and the driven cavity flow are presented. The numerical solutions are obtained for stationary as well as instationary cases and are compared with the analytical solutions for channel flows. Finally, the driven cavity in a unit square is considered and the stationary solution obtained from this scheme is compared with that from the finite element method.
Keywords: Incompressible Navier-Stokes equations, Meshfree method, Projection method, Particle scheme, Least squares approximation
AMS subject classification: 76D05, 76M28
(25 pages, 2001)

31. R. Korn, M. Krekel

Optimal Portfolios with Fixed Consumption or Income Streams

We consider some portfolio optimisation problems where either the investor has a desire for an a priori specified consumption stream or/and follows a deterministic pay in scheme while also trying to maximize expected utility from final wealth. We derive explicit closed form solutions for continuous and discrete monetary streams. The mathematical method used is classical stochastic control theory.
Keywords: Portfolio optimisation, stochastic control, HJB equation, discretisation of control problems.
(23 pages, 2002)

32. M. Krekel

Optimal portfolios with a loan dependent credit spread

If an investor borrows money he generally has to pay higher interest rates than he would have received, if he had put his funds on a savings account. The classical model of continuous time portfolio optimisation ignores this effect. Since there is obviously a connection between the default probability and the total

percentage of wealth, which the investor is in debt, we study portfolio optimisation with a control dependent interest rate. Assuming a logarithmic and a power utility function, respectively, we prove explicit formulae of the optimal control.

Keywords: Portfolio optimisation, stochastic control, HJB equation, credit spread, log utility, power utility, non-linear wealth dynamics
(25 pages, 2002)

33. J. Ohser, W. Nagel, K. Schladitz

The Euler number of discretized sets - on the choice of adjacency in homogeneous lattices

Two approaches for determining the Euler-Poincaré characteristic of a set observed on lattice points are considered in the context of image analysis { the integral geometric and the polyhedral approach. Information about the set is assumed to be available on lattice points only. In order to retain properties of the Euler number and to provide a good approximation of the true Euler number of the original set in the Euclidean space, the appropriate choice of adjacency in the lattice for the set and its background is crucial. Adjacencies are defined using tessellations of the whole space into polyhedrons. In R 3 , two new 14 adjacencies are introduced additionally to the well known 6 and 26 adjacencies. For the Euler number of a set and its complement, a consistency relation holds. Each of the pairs of adjacencies (14:1; 14:1), (14:2; 14:2), (6; 26), and (26; 6) is shown to be a pair of complementary adjacencies with respect to this relation. That is, the approximations of the Euler numbers are consistent if the set and its background (complement) are equipped with this pair of adjacencies. Furthermore, sufficient conditions for the correctness of the approximations of the Euler number are given. The analysis of selected microstructures and a simulation study illustrate how the estimated Euler number depends on the chosen adjacency. It also shows that there is not a uniquely best pair of adjacencies with respect to the estimation of the Euler number of a set in Euclidean space.

Keywords: image analysis, Euler number, neighborhod relationships, cuboidal lattice
(32 pages, 2002)

34. I. Ginzburg, K. Steiner

Lattice Boltzmann Model for Free-Surface flow and Its Application to Filling Process in Casting

A generalized lattice Boltzmann model to simulate free-surface is constructed in both two and three dimensions. The proposed model satisfies the interfacial boundary conditions accurately. A distinctive feature of the model is that the collision processes is carried out only on the points occupied partially or fully by the fluid. To maintain a sharp interfacial front, the method includes an anti-diffusion algorithm. The unknown distribution functions at the interfacial region are constructed according to the first order Chapman-Enskog analysis. The interfacial boundary conditions are satisfied exactly by the coefficients in the Chapman-Enskog expansion. The distribution functions are naturally expressed in the local interfacial coordinates. The macroscopic quantities at the interface are extracted from the least-square solutions of a locally linearized system obtained from the known distribution functions. The proposed method does not require any geometric front construction and is robust for any interfacial topology. Simulation results of realistic filling process are presented: rectangular cavity in two dimensions and Hammer box, Campbell box, Sheffield box, and Motorblock in three dimensions. To enhance the stability at high Reynolds numbers, various upwind-type schemes are developed. Free-slip and no-slip boundary conditions are also discussed.

Keywords: Lattice Boltzmann models; free-surface phenomena; interface boundary conditions; filling processes; injection molding; volume of fluid method; interface boundary conditions; advection-schemes; upwind-schemes
(54 pages, 2002)

35. M. Günther, A. Klar, T. Materne, R. Wegener

Multivalued fundamental diagrams and stop and go waves for continuum traffic equations

In the present paper a kinetic model for vehicular traffic leading to multivalued fundamental diagrams is developed and investigated in detail. For this model phase transitions can appear depending on the local density and velocity of the flow. A derivation of associated macroscopic traffic equations from the kinetic equation is given. Moreover, numerical experiments show the appearance of stop and go waves for highway traffic with a bottleneck.

Keywords: traffic flow, macroscopic equations, kinetic derivation, multivalued fundamental diagram, stop and go waves, phase transitions
(25 pages, 2002)

36. S. Feldmann, P. Lang, D. Prätzel-Wolters

Parameter influence on the zeros of network determinants

To a network N(q) with determinant D(s;q) depending on a parameter vector q Î Rr via identification of some of its vertices, a network N^ (q) is assigned. The paper deals with procedures to find N^ (q), such that its determinant D^ (s;q) admits a factorization in the determinants of appropriate subnetworks, and with the estimation of the deviation of the zeros of D^ from the zeros of D. To solve the estimation problem state space methods are applied.

Keywords: Networks, Equicofactor matrix polynomials, Realization theory, Matrix perturbation theory
(30 pages, 2002)

37. K. Koch, J. Ohser, K. Schladitz

Spectral theory for random closed sets and estimating the covariance via frequency space

A spectral theory for stationary random closed sets is developed and provided with a sound mathematical basis. Definition and proof of existence of the Bartlett spectrum of a stationary random closed set as well as the proof of a Wiener-Khintchine theorem for the power spectrum are used to two ends: First, well known second order characteristics like the covariance can be estimated faster than usual via frequency space. Second, the Bartlett spectrum and the power spectrum can be used as second order characteristics in frequency space. Examples show, that in some cases information about the random closed set is easier to obtain from these characteristics in frequency space than from their real world counterparts.

Keywords: Random set, Bartlett spectrum, fast Fourier transform, power spectrum
(28 pages, 2002)

38. D. d'Humières, I. Ginzburg

Multi-reflection boundary conditions for lattice Boltzmann models

We present a unified approach of several boundary conditions for lattice Boltzmann models. Its general framework is a generalization of previously introduced schemes such as the bounce-back rule, linear or quadratic interpolations, etc. The objectives are two fold: first to give theoretical tools to study the existing boundary conditions and their corresponding accuracy; secondly to design formally third- order accurate boundary conditions for general flows. Using these boundary conditions, Couette and Poiseuille flows are exact solutions of the lattice Boltzmann models for a Reynolds number Re = 0 (Stokes limit).
Numerical comparisons are given for Stokes flows in periodic arrays of spheres and cylinders, linear periodic array of cylinders between moving plates and for Navier-Stokes flows in periodic arrays of cylinders for Re < 200. These results show a significant improvement of the overall accuracy when using the linear interpolations instead of the bounce-back reflection (up to an order of magnitude on the hydrodynamics fields). Further improvement is achieved with the new multi-reflection boundary conditions, reaching a

level of accuracy close to the quasi-analytical reference solutions, even for rather modest grid resolutions and few points in the narrowest channels. More important, the pressure and velocity fields in the vicinity of the obstacles are much smoother with multi-reflection than with the other boundary conditions.
Finally the good stability of these schemes is highlighted by some simulations of moving obstacles: a cylinder between flat walls and a sphere in a cylinder.

Keywords: lattice Boltzmann equation, boudary conditions, bounce-back rule, Navier-Stokes equation
(72 pages, 2002)

39. R. Korn

Elementare Finanzmathematik

Im Rahmen dieser Arbeit soll eine elementar gehaltene Einführung in die Aufgabenstellungen und Prinzipien der modernen Finanzmathematik gegeben werden. Insbesondere werden die Grundlagen der Modellierung von Aktienkursen, der Bewertung von Optionen und der Portfolio-Optimierung vorgestellt. Natürlich können die verwendeten Methoden nicht in voller Allgemeinheit für den Schulunterricht verwendet werden, doch sollen einzelne Prinzipien so heraus gearbeitet werden, dass sie auch an einfachen Beispielen verstanden werden können.

Keywords: Finanzmathematik, Aktien, Optionen, Portfolio-Optimierung, Börse, Lehrerweiterbildung, Mathematikunterricht
(98 pages, 2002)

40. J. Kallrath, M. C. Müller, S. Nickel

Batch Presorting Problems: Models and Complexity Results

In this paper we consider short term storage systems. We analyze presorting strategies to improve the effiency of these storage systems. The presorting task is called Batch PreSorting Problem (BPSP). The BPSP is a variation of an assigment problem, i. e., it has an assigment problem kernel and some additional constraints. We present different types of these presorting problems, introduce mathematical programming formulations and prove the NP-completeness for one type of the BPSP. Experiments are carried out in order to compare the different model formulations and to investigate the behavior of these models.

Keywords: Complexity theory, Integer programming, Assigment, Logistics
(19 pages, 2002)

41. J. Linn

On the frame-invariant description of the phase space of the Folgar-Tucker equation

The Folgar-Tucker equation is used in flow simulations of fiber suspensions to predict fiber orientation depending on the local flow. In this paper, a complete, frame-invariant description of the phase space of this differential equation is presented for the first time.

Key words: fiber orientation, Folgar-Tucker equation, injection molding
(5 pages, 2003)

42. T. Hanne, S. Nickel

A Multi-Objective Evolutionary Algorithm for Scheduling and Inspection Planning in Software Development Projects

In this article, we consider the problem of planning inspections and other tasks within a software development (SD) project with respect to the objectives quality (no. of defects), project duration, and costs. Based on a discrete-event simulation model of SD processes comprising the phases coding, inspection, test, and rework, we present a simplified formulation of the problem as a multiobjective optimization problem. For solving the problem (i. e. finding an approximation of the efficient set) we develop a multiobjective evolutionary algorithm. Details of the algorithm are discussed as well as results of its application to sample problems.

Key words: multiple objective programming, project management and scheduling, software development, evolutionary algorithms, efficient set
(29 pages, 2003)

43. T. Bortfeld, K.-H. Küfer, M. Monz, A. Scherrer, C. Thieke, H. Trinkaus

Intensity-Modulated Radiotherapy - A Large Scale Multi-Criteria Programming Problem -

Radiation therapy planning is always a tight rope walk between dangerous insufficient dose in the target volume and life threatening overdosing of organs at risk. Finding ideal balances between these inherently contradictory goals challenges dosimetrists and physicians in their daily practice. Today's planning systems are typically based on a single evaluation function that measures the quality of a radiation treatment plan. Unfortunately, such a one dimensional approach cannot satisfactorily map the different backgrounds of physicians and the patient dependent necessities. So, too often a time consuming iteration process between evaluation of dose distribution and redefinition of the evaluation function is needed.

In this paper we propose a generic multi-criteria approach based on Pareto's solution concept. For each entity of interest - target volume or organ at risk a structure dependent evaluation function is defined measuring deviations from ideal doses that are calculated from statistical functions. A reasonable bunch of clinically meaningful Pareto optimal solutions are stored in a data base, which can be interactively searched by physicians. The system guarantees dynamical planning as well as the discussion of tradeoffs between different entities.

Mathematically, we model the upcoming inverse problem as a multi-criteria linear programming problem. Because of the large scale nature of the problem it is not possible to solve the problem in a 3D-setting without adaptive reduction by appropriate approximation schemes.

Our approach is twofold: First, the discretization of the continuous problem is based on an adaptive hierarchical clustering process which is used for a local refinement of constraints during the optimization procedure. Second, the set of Pareto optimal solutions is approximated by an adaptive grid of representatives that are found by a hybrid process of calculating extreme compromises and interpolation methods.

Keywords: multiple criteria optimization, representative systems of Pareto solutions, adaptive triangulation, clustering and disaggregation techniques, visualization of Pareto solutions, medical physics, external beam radiotherapy planning, intensity modulated radiotherapy

(31 pages, 2003)

44. T. Halfmann, T. Wichmann

Overview of Symbolic Methods in Industrial Analog Circuit Design

Industrial analog circuits are usually designed using numerical simulation tools. To obtain a deeper circuit understanding, symbolic analysis techniques can additionally be applied. Approximation methods which reduce the complexity of symbolic expressions are needed in order to handle industrial-sized problems. This paper will give an overview to the field of symbolic analog circuit analysis. Starting with a motivation, the state-of-the-art simplification algorithms for linear as well as for nonlinear circuits are presented. The basic ideas behind the different techniques are described, whereas the technical details can be found in the cited references. Finally, the application of linear and nonlinear symbolic analysis will be shown on two example circuits.

Keywords: CAD, automated analog circuit design, symbolic analysis, computer algebra, behavioral modeling, system simulation, circuit sizing, macro modeling, differential-algebraic equations, index

(17 pages, 2003)

45. S. E. Mikhailov, J. Orlik

Asymptotic Homogenisation in Strength and Fatigue Durability Analysis of Composites

Asymptotic homogenisation technique and two-scale convergence is used for analysis of macro-strength and fatigue durability of composites with a periodic structure under cyclic loading. The linear damage accumulation rule is employed in the phenomenological micro-durability conditions (for each component of the composite) under varying cyclic loading. Both local and non-local strength and durability conditions are analysed. The strong convergence of the strength and fatigue damage measure as the structure period tends to zero is proved and their limiting values are estimated.

Keywords: multiscale structures, asymptotic homogenization, strength, fatigue, singularity, non-local conditions

(14 pages, 2003)

46. P. Domínguez-Marín, P. Hansen, N. Mladenović, S. Nickel

Heuristic Procedures for Solving the Discrete Ordered Median Problem

We present two heuristic methods for solving the Discrete Ordered Median Problem (DOMP), for which no such approaches have been developed so far. The DOMP generalizes classical discrete facility location problems, such as the p-median, p-center and Uncapacitated Facility Location problems. The first procedure proposed in this paper is based on a genetic algorithm developed by Moreno Vega [MV96] for p-median and p-center problems. Additionally, a second heuristic approach based on the Variable Neighborhood Search metaheuristic (VNS) proposed by Hansen & Mladenovic [HM97] for the p-median problem is described. An extensive numerical study is presented to show the efficiency of both heuristics and compare them.

Keywords: genetic algorithms, variable neighborhood search, discrete facility location

(31 pages, 2003)

47. N. Boland, P. Domínguez-Marín, S. Nickel, J. Puerto

Exact Procedures for Solving the Discrete Ordered Median Problem

The Discrete Ordered Median Problem (DOMP) generalizes classical discrete location problems, such as the N-median, N-center and Uncapacitated Facility Location problems. It was introduced by Nickel [16], who formulated it as both a nonlinear and a linear integer program. We propose an alternative integer linear programming formulation for the DOMP, discuss relationships between both integer linear programming formulations, and show how properties of optimal solutions can be used to strengthen these formulations. Moreover, we present a specific branch and bound procedure to solve the DOMP more efficiently. We test the integer linear programming formulations and this branch and bound method computationally on randomly generated test problems.

Keywords: discrete location, Integer programming

(41 pages, 2003)

48. S. Feldmann, P. Lang

Padé-like reduction of stable discrete linear systems preserving their stability

A new stability preserving model reduction algorithm for discrete linear SISO-systems based on their impulse response is proposed. Similar to the Padé approximation, an equation system for the Markov parameters involving the Hankel matrix is considered, that here however is chosen to be of very high dimension. Although this equation system therefore in general cannot be solved exactly, it is proved that the approximate solution, computed via the Moore-Penrose inverse, gives rise to a stability preserving reduction scheme, a property that cannot be guaranteed for the Padé approach. Furthermore, the proposed algorithm is compared to another stability preserving reduction approach, namely the balanced truncation method, showing comparable performance of the reduced systems. The balanced truncation method however starts from a state space description of the systems and in general is expected to be more computational demanding.

Keywords: Discrete linear systems, model reduction, stability, Hankel matrix, Stein equation

(16 pages, 2003)

49. J. Kallrath, S. Nickel

A Polynomial Case of the Batch Presorting Problem

This paper presents new theoretical results for a special case of the batch presorting problem (BPSP). We will show tht this case can be solved in polynomial time. Offline and online algorithms are presented for solving the BPSP. Competetive analysis is used for comparing the algorithms.

Keywords: batch presorting problem, online optimization, competetive analysis, polynomial algorithms, logistics

(17 pages, 2003)

50. T. Hanne, H. L. Trinkaus

knowCube for MCDM – Visual and Interactive Support for Multicriteria Decision Making

In this paper, we present a novel multicriteria decision support system (MCDSS), called knowCube, consisting of components for knowledge organization, generation, and navigation. Knowledge organization rests upon a database for managing qualitative and quantitative criteria, together with add-on information. Knowledge generation serves filling the database via e. g. identification, optimization, classification or simulation. For "finding needles in haycocks", the knowledge navigation component supports graphical database retrieval and interactive, goal-oriented problem solving. Navigation "helpers" are, for instance, cascading criteria aggregations, modifiable metrics, ergonomic interfaces, and customizable visualizations. Examples from real-life projects, e.g. in industrial engineering and in the life sciences, illustrate the application of our MCDSS.

Key words: Multicriteria decision making, knowledge management, decision support systems, visual interfaces, interactive navigation, real-life applications.

(26 pages, 2003)

51. O. Iliev, V. Laptev

On Numerical Simulation of Flow Through Oil Filters

This paper concerns numerical simulation of flow through oil filters. Oil filters consist of filter housing (filter box), and a porous filtering medium, which completely separates the inlet from the outlet. We discuss mathematical models, describing coupled flows in the pure liquid subregions and in the porous filter media, as well as interface conditions between them. Further, we reformulate the problem in fictitious regions method manner, and discuss peculiarities of the numerical algorithm in solving the coupled system. Next, we show numerical results, validating the model and the algorithm. Finally, we present results from simulation of 3-D oil flow through a real car filter.

Keywords: oil filters, coupled flow in plain and porous media, Navier-Stokes, Brinkman, numerical simulation

(8 pages, 2003)

52. W. Dörfler, O. Iliev, D. Stoyanov, D. Vassileva

On a Multigrid Adaptive Refinement Solver for Saturated Non-Newtonian Flow in Porous Media

A multigrid adaptive refinement algorithm for non-Newtonian flow in porous media is presented. The saturated flow of a non-Newtonian fluid is described by the continuity equation and the generalized Darcy law. The resulting second order nonlinear elliptic equation is discretized by a finite volume method on a cell-centered grid. A nonlinear full-multigrid, full-approximation-storage algorithm is implemented. As a smoother, a single grid solver based on Picard linearization and Gauss-Seidel relaxation is used. Further, a local refinement multigrid algorithm on a composite grid is developed. A residual based error indicator is used in the adaptive refinement criterion. A special implementation approach is used, which allows us to perform unstructured local refinement in conjunction with the finite volume discretization. Several results from numerical experiments are presented in order to examine the performance of the solver.

Keywords: Nonlinear multigrid, adaptive refinement, non-Newtonian flow in porous media

(17 pages, 2003)

53. S. Kruse

On the Pricing of Forward Starting Options under Stochastic Volatility

We consider the problem of pricing European forward starting options in the presence of stochastic volatility. By performing a change of measure using the asset price at the time of strike determination as a numeraire, we derive a closed-form solution based on Heston's model of stochastic volatility.

Keywords: Option pricing, forward starting options, Heston model, stochastic volatility, cliquet options

(11 pages, 2003)

54. O. Iliev, D. Stoyanov

Multigrid – adaptive local refinement solver for incompressible flows

A non-linear multigrid solver for incompressible Navier-Stokes equations, exploiting finite volume discretization of the equations, is extended by adaptive local refinement. The multigrid is the outer iterative cycle, while the SIMPLE algorithm is used as a smoothing procedure. Error indicators are used to define the refinement subdomain. A special implementation approach is used, which allows to perform unstructured local refinement in conjunction with the finite volume discretization. The multigrid - adaptive local refinement algorithm is tested on 2D Poisson equation and further is applied to a lid-driven flows in a cavity (2D and 3D case), comparing the results with bench-mark data. The software design principles of the solver are also discussed.

Keywords: Navier-Stokes equations, incompressible flow, projection-type splitting, SIMPLE, multigrid methods, adaptive local refinement, lid-driven flow in a cavity

(37 pages, 2003)

55. V. Starikovicius

The multiphase flow and heat transfer in porous media

In first part of this work, summaries of traditional Multiphase Flow Model and more recent Multiphase Mixture Model are presented. Attention is being paid to attempts include various heterogeneous aspects into models. In second part, MMM based differential model for two-phase immiscible flow in porous media is considered. A numerical scheme based on the sequential solution procedure and control volume based finite difference schemes for the pressure and saturation-conservation equations is developed. A computer simulator is built, which exploits object-oriented programming techniques. Numerical result for several test problems are reported.

Keywords: Two-phase flow in porous media, various formulations, global pressure, multiphase mixture model, numerical simulation

(30 pages, 2003)

56. P. Lang, A. Sarishvili, A. Wirsen

Blocked neural networks for knowledge extraction in the software development process

One of the main goals of an organization developing software is to increase the quality of the software while at the same time to decrease the costs and the duration of the development process. To achieve this, various decisions e.ecting this goal before and during the development process have to be made by the managers. One appropriate tool for decision support are simulation models of the software life cycle, which also help to understand the dynamics of the software development process. Building up a simulation model requires a mathematical description of the interactions between di.erent objects involved in the development process. Based on experimental data, techniques from the .eld of knowledge discovery can be used to quantify these interactions and to generate new process knowledge based on the analysis of the determined relationships. In this paper blocked neuronal networks and related relevance measures will be presented as an appropriate tool for quanti.cation and validation of qualitatively known dependencies in the software development process.

Keywords: Blocked Neural Networks, Nonlinear Regression, Knowledge Extraction, Code Inspection

(21 pages, 2003)

57. H. Knaf, P. Lang, S. Zeiser

Diagnosis aiding in Regulation Thermography using Fuzzy Logic

The objective of the present article is to give an overview of an application of Fuzzy Logic in Regulation Thermography, a method of medical diagnosis support. An introduction to this method of the complementary medical science based on temperature measurements – so-called thermograms – is provided. The process of modelling the physician's thermogram evaluation rules using the calculus of Fuzzy Logic is explained.

Keywords: fuzzy logic,knowledge representation, expert system

(22 pages, 2003)

58. M.T. Melo, S. Nickel, F. Saldanha da Gama

Largescale models for dynamic multi-commodity capacitated facility location

In this paper we focus on the strategic design of supply chain networks. We propose a mathematical modeling framework that captures many practical aspects of network design problems simultaneously but which have not received adequate attention in the literature. The aspects considered include: dynamic planning horizon, generic supply chain network structure, external supply of materials, inventory opportunities for goods, distribution of commodities, facility configuration, availability of capital for investments, and storage limitations. Moreover, network configuration decisions concerning the gradual relocation of facilities over the planning horizon are considered. To cope with fluctuating demands, capacity expansion and reduction scenarios are also analyzed as well as modular capacity shifts. The relation of the proposed modeling framework with existing models is discussed. For problems of reasonable size we report on our computational experience with standard mathematical programming software. In particular, useful insights on the impact of various factors on network design decisions are provided.

Keywords: supply chain management, strategic planning, dynamic location, modeling

(40 pages, 2003)

59. J. Orlik

Homogenization for contact problems with periodically rough surfaces

We consider the contact of two elastic bodies with rough surfaces at the interface. The size of the micropeaks and valleys is very small compared with the macrosize of the bodies' domains. This makes the direct application of the FEM for the calculation of the contact problem prohibitively costly. A method is developed that allows deriving a macrocontact condition on the interface. The method involves the twoscale asymptotic homogenization procedure that takes into account the microgeometry of the interface layer and the stiffnesses of materials of both domains. The macrocontact condition can then be used in a FEM model for the contact problem on the macrolevel. The averaged contact stiffness obtained allows the replacement of the interface layer in the macromodel by the macrocontact condition.

Keywords: asymptotic homogenization, contact problems

(28 pages, 2004)

60. A. Scherrer, K.-H. Küfer, M. Monz, F. Alonso, T. Bortfeld

IMRT planning on adaptive volume structures – a significant advance of computational complexity

In intensity-modulated radiotherapy (IMRT) planning the oncologist faces the challenging task of finding a treatment plan that he considers to be an ideal compromise of the inherently contradictive goals of delivering a sufficiently high dose to the target while widely sparing critical structures. The search for this a priori unknown compromise typically requires the computation of several plans, i.e. the solution of several optimization problems. This accumulates to a high computational expense due to the large scale of these problems - a consequence of the discrete problem formulation. This paper presents the adaptive clustering method as a new algorithmic concept to overcome these difficulties. The computations are performed on an individually adapted structure of voxel clusters rather than on the original voxels leading to a decisively reduced computational complexity as numerical examples on real clinical data demonstrate. In contrast to many other similar concepts, the typical trade-off between a reduction in computational complexity and a loss in exactness can be avoided: the adaptive clustering method produces the optimum of the original problem. This flexible method can be applied to both single- and multi-criteria optimization methods based on most of the convex evaluation functions used in practice.

Keywords: Intensity-modulated radiation therapy (IMRT), inverse treatment planning, adaptive volume structures, hierarchical clustering, local refinement, adaptive clustering, convex programming, mesh generation, multi-grid methods

(24 pages, 2004)

61. D. Kehrwald

Parallel lattice Boltzmann simulation of complex flows

After a short introduction to the basic ideas of lattice Boltzmann methods and a brief description of a modern parallel computer, it is shown how lattice Boltzmann schemes are successfully applied for simulating fluid flow in microstructures and calculating material properties of porous media. It is explained how lattice Boltzmann schemes compute the gradient of the velocity field without numerical differentiation. This feature is then utilised for the simulation of pseudo-plastic fluids, and numerical results are presented for a simple benchmark problem as well as for the simulation of liquid composite moulding.

Keywords: Lattice Boltzmann methods, parallel computing, microstructure simulation, virtual material design, pseudo-plastic fluids, liquid composite moulding

(12 pages, 2004)

62. O. Iliev, J. Linn, M. Moog, D. Niedziela, V. Starikovicius

On the Performance of Certain Iterative Solvers for Coupled Systems Arising in Discretization of Non-Newtonian Flow Equations

Iterative solution of large scale systems arising after discretization and linearization of the unsteady non-Newtonian Navier–Stokes equations is studied. cross WLF model is used to account for the non-Newtonian behavior of the fluid. Finite volume method is used to discretize the governing system of PDEs. Viscosity is treated explicitly (e.g., it is taken from the previous time step), while other terms are treated implicitly. Different preconditioners (block–diagonal, block–triangular, relaxed incomplete LU factorization, etc.) are used in conjunction with advanced iterative methods, namely, BiCGStab, CGS, GMRES. The action of the preconditioner in fact requires inverting different blocks. For this purpose, in addition to preconditioned BiCGStab, CGS, GMRES, we use also algebraic multigrid method (AMG). The performance of the iterative solvers is studied with respect to the number of unknowns, characteristic velocity in the basic flow, time step, deviation from Newtonian behavior, etc. Results from numerical experiments are presented and discussed.

Keywords: Performance of iterative solvers, Preconditioners, Non-Newtonian flow

(17 pages, 2004)

63. R. Ciegis, O. Iliev, S. Rief, K. Steiner

On Modelling and Simulation of Different Regimes for Liquid Polymer Moulding

In this paper we consider numerical algorithms for solving a system of nonlinear PDEs arising in modeling of liquid polymer injection. We investigate the particular case when a porous preform is located within the mould, so that the liquid polymer flows through a porous medium during the filling stage. The nonlinearity of the governing system of PDEs is due to the non-Newtonian behavior of the polymer, as well as due to the moving free boundary. The latter is related to the penetration front and a Stefan type problem is formulated to account for it. A finite-volume method is used

to approximate the given differential problem. Results of numerical experiments are presented.

We also solve an inverse problem and present algorithms for the determination of the absolute preform permeability coefficient in the case when the velocity of the penetration front is known from measurements. In both cases (direct and inverse problems) we emphasize on the specifics related to the non-Newtonian behavior of the polymer. For completeness, we discuss also the Newtonian case. Results of some experimental measurements are presented and discussed.

Keywords: Liquid Polymer Moulding, Modelling, Simulation, Infiltration, Front Propagation, non-Newtonian flow in porous media

(43 pages, 2004)

64. T. Hanne, H. Neu

Simulating Human Resources in Software Development Processes

In this paper, we discuss approaches related to the explicit modeling of human beings in software development processes. While in most older simulation models of software development processes, esp. those of the system dynamics type, humans are only represented as a labor pool, more recent models of the discrete-event simulation type require representations of individual humans. In that case, particularities regarding the person become more relevant. These individual effects are either considered as stochastic variations of productivity, or an explanation is sought based on individual characteristics, such as skills for instance. In this paper, we explore such possibilities by recurring to some basic results in psychology, sociology, and labor science. Various specific models for representing human effects in software process simulation are discussed.

Keywords: Human resource modeling, software process, productivity, human factors, learning curve

(14 pages, 2004)

65. O. Iliev, A. Mikelic, P. Popov

Fluid structure interaction problems in deformable porous media: Toward permeability of deformable porous media

In this work the problem of fluid flow in deformable porous media is studied. First, the stationary fluid-structure interaction (FSI) problem is formulated in terms of incompressible Newtonian fluid and a linearized elastic solid. The flow is assumed to be characterized by very low Reynolds number and is described by the Stokes equations. The strains in the solid are small allowing for the solid to be described by the Lame equations, but no restrictions are applied on the magnitude of the displacements leading to strongly coupled, nonlinear fluid-structure problem. The FSI problem is then solved numerically by an iterative procedure which solves sequentially fluid and solid subproblems. Each of the two subproblems is discretized by finite elements and the fluid-structure coupling is reduced to an interface boundary condition. Several numerical examples are presented and the results from the numerical computations are used to perform permeability computations for different geometries.

Keywords: fluid-structure interaction, deformable porous media, upscaling, linear elasticity, stokes, finite elements

(23 pages, 2004)

66. F. Gaspar, O. Iliev, F. Lisbona, A. Naumovich, P. Vabishchevich

On numerical solution of 1-D poroelasticity equations in a multilayered domain

Finite volume discretization of Biot system of poroelasticity in a multilayered domain is presented. Staggered grid is used in order to avoid nonphysical oscillations of the numerical solution, appearing when a collocated grid is used. Various numerical experiments are presented in order to illustrate the accuracy of the finite difference scheme. In the first group of experiments, problems having analytical solutions are solved, and the order of convergence for the velocity, the pressure, the displacements, and the stresses is analyzed. In the second group of experiments numerical solution of real problems is presented.

Keywords: poroelasticity, multilayered material, finite volume discretization, MAC type grid

(41 pages, 2004)

67. J. Ohser, K. Schladitz, K. Koch, M. Nöthe

Diffraction by image processing and its application in materials science

A spectral theory for constituents of macroscopically homogeneous random microstructures modeled as homogeneous random closed sets is developed and provided with a sound mathematical basis, where the spectrum obtained by Fourier methods corresponds to the angular intensity distribution of x-rays scattered by this constituent. It is shown that the fast Fourier transform applied to three-dimensional images of microstructures obtained by micro-tomography is a powerful tool of image processing. The applicability of this technique is is demonstrated in the analysis of images of porous media.

Keywords: porous microstructure, image analysis, random set, fast Fourier transform, power spectrum, Bartlett spectrum

(13 pages, 2004)

68. H. Neunzert

Mathematics as a Technology: Challenges for the next 10 Years

No doubt: Mathematics has become a technology in its own right, maybe even a key technology. Technology may be defined as the application of science to the problems of commerce and industry. And science? Science maybe defined as developing, testing and improving models for the prediction of system behavior; the language used to describe these models is mathematics and mathematics provides methods to evaluate these models. Here we are! Why has mathematics become a technology only recently? Since it got a tool, a tool to evaluate complex, "near to reality" models: Computer! The model may be quite old – Navier-Stokes equations describe flow behavior rather well, but to solve these equations for realistic geometry and higher Reynolds numbers with sufficient precision is even for powerful parallel computing a real challenge. Make the models as simple as possible, as complex as necessary – and then evaluate them with the help of efficient and reliable algorithms: These are genuine mathematical tasks.

Keywords: applied mathematics, technology, modelling, simulation, visualization, optimization, glass processing, spinning processes, fiber-fluid interaction, trubulence effects, topological optimization, multicriteria optimization, Uncertainty and Risk, financial mathematics, Malliavin calculus, Monte-Carlo methods, virtual material design, filtration, bio-informatics, system biology

(29 pages, 2004)

69. R. Ewing, O. Iliev, R. Lazarov, A. Naumovich

On convergence of certain finite difference discretizations for 1D poroelasticity interface problems

Finite difference discretizations of 1D poroelasticity equations with discontinuous coefficients are analyzed. A recently suggested FD discretization of poroelasticity equations with constant coefficients on staggered grid, [5], is used as a basis. A careful treatment of the interfaces leads to harmonic averaging of the discontinuous coefficients. Here, convergence for the pressure and for the displacement are proven in certain norms for the scheme with harmonic averaging (HA). Order of convergence 1.5 is proven for arbitrary located interface, and second order convergence is proven for the case when the interface coincides with a grid node. Furthermore, following the ideas from [3], modified HA discretization are suggested for particular cases. The velocity and the stress are approximated with second order on the interface in this case. It is shown that for wide class of problems, the modified discretization provides better accuracy. Second order convergence for modified scheme is proven for the case when the interface coincides with a displacement grid node. Numerical experiments are presented in order to illustrate our considerations.

Keywords: poroelasticity, multilayered material, finite volume discretizations, MAC type grid, error estimates

(26 pages,2004)

70. W. Dörfler, O. Iliev, D. Stoyanov, D. Vassileva

On Efficient Simulation of Non-Newtonian Flow in Saturated Porous Media with a Multigrid Adaptive Refinement Solver

Flow of non-Newtonian in saturated porous media can be described by the continuity equation and the generalized Darcy law. Efficient solution of the resulting second order nonlinear elliptic equation is discussed here. The equation is discretized by a finite volume method on a cell-centered grid. Local adaptive refinement of the grid is introduced in order to reduce the number of unknowns. A special implementation approach is used, which allows us to perform unstructured local refinement in conjunction with the finite volume discretization. Two residual based error indicators are exploited in the adaptive refinement criterion. Second order accurate discretization on the interfaces between refined and non-refined subdomains, as well as on the boundaries with Dirichlet boundary condition, are presented here, as an essential part of the accurate and efficient algorithm. A nonlinear full approximation storage multigrid algorithm is developed especially for the above described composite (coarse plus locally refined) grid approach. In particular, second order approximation around interfaces is a result of a quadratic approximation of slave nodes in the multigrid - adaptive refinement (MG-AR) algorithm. Results from numerical solution of various academic and practice-induced problems are presented and the performance of the solver is discussed.

Keywords: Nonlinear multigrid, adaptive renement, non-Newtonian in porous media

(25 pages, 2004)

71. J. Kalcsics, S. Nickel, M. Schröder

Towards a Unified Territory Design Approach – Applications, Algorithms and GIS Integration

Territory design may be viewed as the problem of grouping small geographic areas into larger geographic clusters called territories in such a way that the latter are acceptable according to relevant planning criteria. In this paper we review the existing literature for applications of territory design problems and solution approaches for solving these types of problems. After identifying features common to all applications we introduce a basic territory design model and present in detail two approaches for solving this model: a classical location–allocation approach combined with optimal split resolution techniques and a newly developed computational geometry based method. We present computational results indicating the efficiency and suitability of the latter method for solving large–scale practical problems in an interactive environment. Furthermore, we discuss extensions to the basic model and its integration into Geographic Information Systems.

Keywords: territory desgin, political districting, sales territory alignment, optimization algorithms, Geographical Information Systems

(40 pages, 2005)

72. K. Schladitz, S. Peters, D. Reinel-Bitzer, A. Wiegmann, J. Ohser

Design of acoustic trim based on geometric modeling and flow simulation for non-woven

In order to optimize the acoustic properties of a stacked fiber non-woven, the microstructure of the non-woven is modeled by a macroscopically homogeneous random system of straight cylinders (tubes). That is, the fibers are modeled by a spatially stationary random system of lines (Poisson line process), dilated by a sphere. Pressing the non-woven causes anisotropy. In our model, this anisotropy is described by a one parametric distribution of the direction of the fibers. In the present application, the anisotropy parameter has to be estimated from 2d reflected light microscopic images of microsections of the non-woven.

After fitting the model, the flow is computed in digitized realizations of the stochastic geometric model using the lattice Boltzmann method. Based on the flow resistivity, the formulas of Delany and Bazley predict the frequency-dependent acoustic absorption of the non-woven in the impedance tube.

Using the geometric model, the description of a non-woven with improved acoustic absorption properties is obtained in the following way: First, the fiber thicknesses, porosity and anisotropy of the fiber system are modified. Then the flow and acoustics simulations are performed in the new sample. These two steps are repeatedc for various sets of parameters. Finally, the set of parameters for the geometric model leading to the best acoustic absorption is chosen.

Keywords: random system of fibers, Poisson line process, flow resistivity, acoustic absorption, Lattice-Boltzmann method, non-woven

(21 pages, 2005)

73. V. Rutka, A. Wiegmann

Explicit Jump Immersed Interface Method for virtual material design of the effective elastic moduli of composite materials

Virtual material design is the microscopic variation of materials in the computer, followed by the numerical evaluation of the effect of this variation on the material's macroscopic properties. The goal of this procedure is an in some sense improved material. Here, we give examples regarding the dependence of the effective elastic moduli of a composite material on the geometry of the shape of an inclusion. A new approach on how to solve such interface problems avoids mesh generation and gives second order accurate results even in the vicinity of the interface.

The Explicit Jump Immersed Interface Method is a finite difference method for elliptic partial differential equations that works on an equidistant Cartesian grid in spite of non-grid aligned discontinuities in equation parameters and solution. Near discontinuities, the standard finite difference approximations are modified by adding correction terms that involve jumps in the function and its derivatives. This work derives the correction terms for two dimensional linear elasticity with piecewise constant coefficients, i.e. for composite materials. It demonstrates numerically convergence and approximation properties of the method.

Keywords: virtual material design, explicit jump immersed interface method, effective elastic moduli, composite materials

(22 pages, 2005)

74. T. Hanne

Eine Übersicht zum Scheduling von Baustellen

Im diesem Dokument werden Aspekte der formalen zeitlichen Planung bzw. des Scheduling für Bauprojekte anhand ausgewählter Literatur diskutiert. Auf allgemeine Aspekte des Scheduling soll dabei nicht eingegangen werden. Hierzu seien als Standard-Referenzen nur Brucker (2004) und Pinedo (1995) genannt. Zu allgemeinen Fragen des Projekt-Managements sei auf Kerzner (2003) verwiesen.

Im Abschnitt 1 werden einige Anforderungen und Besonderheiten der Planung von Baustellen diskutiert. Diese treten allerdings auch in zahlreichen anderen Bereichen der Produktionsplanung und des Projektmanagements auf. In Abschnitt 2 werden dann Aspekte zur Formalisierung von Scheduling-Problemen in der Bauwirtschaft diskutiert, insbesondere Ziele und zu berücksichtigende Restriktionen. Auf eine mathematische Formalisierung wird dabei allerdings verzichtet. Abschnitt 3 bietet eine Übersicht über Verfahren und grundlegende Techniken für die Berechnung von Schedules. In Abschnitt 4 wird ein Überblick über vorhandene Software, zum einen verbreitete Internationale Software, zum anderen deutschsprachige Branchenlösungen, gegeben. Anschließend werden Schlussfolgerungen gezogen und es erfolgt eine Auflistung der Literaturquellen.

Keywords: Projektplanung, Scheduling, Bauplanung, Bauindustrie

(32 pages, 2005)

Status quo: March 2005